Polymer depletion effects near mesoscopic particles

A. Hanke,[1] E. Eisenriegler,[2] and S. Dietrich[1]

[1]*Fachbereich Physik, Bergische Universität Wuppertal, D-42097 Wuppertal, Federal Republic of Germany*
[2]*Institut für Festkörperforschung, Forschungszentrum Jülich, D-52425 Jülich, Federal Republic of Germany*
(Received 20 August 1998)

The behavior of mesoscopic particles dissolved in a dilute solution of long, flexible, and nonadsorbing polymer chains is studied by field-theoretic methods. For spherical and cylindrical particles the solvation free energy for immersing a single particle in the solution is calculated explicitly. Important features are qualitatively different for self-avoiding polymer chains as compared with ideal chains. The results corroborate the validity of the Helfrich-type curvature expansion for general particle shapes and allow for quantitative experimental tests. For the effective interactions between a small sphere and a wall, between a thin rod and a wall, and between two small spheres, quantitative results are presented. A systematic approach for studying effective many-body interactions is provided. The common Asakura-Oosawa approximation modeling the polymer coils as hard spheres turns out to fail completely for small particles and still fails by about 10% for large particles. [S1063-651X(99)01406-3]

PACS number(s): 61.25.Hq, 05.70.Jk, 68.35.Rh, 82.70.Dd

I. INTRODUCTION

In colloidal suspensions the depletion interaction between mesoscopic dissolved particles and nonadsorbing free polymer chains represents one of the basic and tunable effective interactions (see, e.g., Ref. [1] for a review). For example, adding free polymer chains to the solvent of a colloidal solution leads to an effective attraction between the particles which may lead to flocculation [2]. For two individual colloidal particles or for a single particle near a planar wall this effective interaction can be measured even directly [3,4]. In view of its importance it is surprising that for a long time the interaction between polymers and colloidal particles has been modeled only rather crudely by approximating the polymer chains by nondeformable hard spheres [5,1,3,4].

Chain flexibility has been taken into account only more recently. Mainly the following two cases have been considered: (a) strongly overlapping chains (semidilute solution) which are described within a self-consistent field theory or within the framework of a phenomenological scaling theory [6–9]; (b) nonoverlapping chains (dilute solution) which to a certain extent can be modeled by random walks without self-avoidance (ideal chains) [10–14]. In three dimensions this latter situation is closely realized in a theta solvent [15].

Besides presenting some new results for ideal chains, the main emphasis of the present contribution is on the generic case of a *good* solvent and we investigate systematically the consequences of the ensuing excluded volume interaction (EV interaction) [16] on depletion effects in a dilute and monodisperse polymer solution. The interaction of *long* flexible chains with mesoscopic particles leads to *universal* results which are independent of most microscopic details [15,17–19] and depend only on a few gross properties such as the shape of the particles. By focusing on such systems we obtain results which are free of nonuniversal model parameters. Due to the universality of the corresponding properties it is sufficient to choose a simple model for calculating these results. For example, in a lattice model the interaction between a particle and a nonadsorbing chain can be implemented as the purely geometrical restriction that the chain must not intersect the particle [12]. For our investigations we use an Edwards-type model [15,17,18] for the polymer chain which allows for an expansion in terms of the EV interaction and which is amenable to a field-theoretical treatment. The basic elements in this expansion are partition functions $Z_{[0]}(\mathbf{r},\mathbf{r}')$ for chain segments without EV interaction (as indicated by the subscript $[0]$) and with the two ends of the segment fixed at $\mathbf{r}$ and $\mathbf{r}'$. In this coarse grained description the interaction of the nonadsorbing polymer with the particle is implemented by the boundary condition that the segment partition function vanishes as $\mathbf{r}$ or $\mathbf{r}'$ approaches the surface S of the particle [15,19], i.e.,

$$Z_{[0]}(\mathbf{r},\mathbf{r}') \to 0, \quad \mathbf{r} \to S. \tag{1.1}$$

Equation (1.1) also applies for long walks on a lattice which must not visit the region occupied by the mesoscopic particle [12] provided one considers the variation of the partition function on length scales much larger than the lattice constant.

The only relevant property which characterizes one of the interacting polymer chains is its mean square end-to-end distance $\mathcal{R}_E^2$ in the absence of particles and other chains. Within the perturbative treatment of the EV interaction it will be necessary to generalize the three-dimensional space to a space of D spatial dimensions. In this respect it is convenient [17] to introduce

$$\mathcal{R}_x^2 = \mathcal{R}_E^2/D, \tag{1.2}$$

the mean square of the projection of the end-to-end distance vector onto a particular direction, say, the x axis, in the D-dimensional space. For industrially produced polymers such as polystyrene, values of $\mathcal{R}_x$ up to the order of μm are easily accessible.

The simplest particle shapes relevant for applications are spheres and rods [1] but the particles can also have more complex structures such as those of closed bilayer mem-

branes in the case of vesicles [20]. We note that the radius R of spherical particles can be quite small as compared to accessible values of $\mathcal{R}_x$, e.g., $R \approx 0.012$ μm in the case of Ludox silica particles [21]. Rodlike objects are provided, e.g., by fibers or colloidal rods [22], semiflexible polymers with a large persistence length ℓ_p such as actin for which $\ell_p \approx 17$ μm [23], and microtubuli [23]. The ratio of the length l and the radius R of rodlike particles may be of the order of 40 or larger, in conjunction with a quite small radius such as $R \approx 0.007$ μm in the case of colloidal boehmite rods [22]. As the interaction between rodlike particles and polymers is concerned, we consider *long* rods, i.e., $R, \mathcal{R}_x \ll l$, and neglect effects which may arise due to their finite length l. In order to be able to treat spheres and cylinders in a unified way and in general dimensionality, we are thus led to consider a *generalized cylinder* K with an infinitely extended ''axis'' of dimension δ. Such a generalized cylinder has been introduced in Ref. [14], hereafter denoted as I. The ''axis'' can be the axis of an ordinary infinitely elongated cylinder ($\delta = 1$), or the midplane of a slab ($\delta = D - 1$), or the center of a sphere ($\delta = 0$). For general integer D and δ the explicit form of K is

$$K = \{\mathbf{r} = (\mathbf{r}_\perp, \mathbf{r}_\parallel) \in \mathbb{R}^{D-\delta} \times \mathbb{R}^{\delta}; |\mathbf{r}_\perp| \leqslant R\} \qquad (1.3)$$

with $\mathbf{r}_\perp$ and $\mathbf{r}_\parallel$ perpendicular and parallel to the axis, respectively. Note that $\mathbf{r}_\perp$ is a d-dimensional vector with

$$d = D - \delta. \qquad (1.4)$$

The radius R of the generalized cylinder K is the radius in the cases of an ordinary cylinder or a sphere and it is half of the thickness in the case of a slab. For the slab the geometry reduces to the much studied case of (two decoupled) half spaces [19]. We stress that the generalization of D to values different from 3 is introduced only for technical reasons because $D_{uc} = 4$ marks the upper critical dimension for the relevance of the EV interaction in the bulk [15,17,18]. Eventually we will be interested in—and will obtain results for—the experimentally relevant case $D = 3$. These results concern the solvation free energy for a single particle and the depletion interaction between particles.

A. Solvation free energy of a particle

We consider the increase in configurational free energy of a dilute solution of long flexible polymers with number density n_p upon immersing a single particle. For $\delta > 0$ we actually consider a generalized cylinder with a large but *finite* axis length l^δ (i.e., an ordinary cylinder with axis length l or a slab with cross section area l^{D-1}) and study the increase $n_p f_K^{(1)}$ in free energy per $k_B T$ and per l^δ in the limit $l \to \infty$, for which l drops out [24]. For a sphere $n_p f_K^{(1)}$ is simply the free energy increase per $k_B T$. The additional increase in free energy upon immersing the particle in the polymer-free (i.e., $n_p = 0$) solvent is regarded as a background term which, in an experiment, can be determined separately. In the asymptotic regime where both $\mathcal{R}_x$ and R are large on the microscopic scale (such as the monomer length or the diameter of the solvent molecules) it turns out that $f_K^{(1)}$ takes the scaling form

$$f_K^{(1)} = R^d Y_{d,D}(x), \qquad (1.5)$$

where $Y_{d,D}$ is a universal scaling function of the scaling variable

$$x = \mathcal{R}_x / R. \qquad (1.6)$$

For ideal chains (no EV interaction) and d fixed the function $Y_{d,D} = Y_d^{(id)}$ is independent of D (compare I where $f_K^{(1)}$ was denoted as δf_K). Results for $Y_d^{(id)}$ for $d = 3$ (sphere) and $d = 2$ (cylinder) have been given in Ref. [11] and in I. Here we calculate the scaling function $Y_{d,D}(x)$ for chains with EV interaction perturbatively in terms of $\varepsilon = 4 - D$ with the upper critical dimension $D_{uc} = 4$. In particular, we investigate the following features of $f_K^{(1)}$.

(a) For *short* chains, i.e., $x \ll 1$, we assume that $Y_{d,D}(x)$ is analytic so that it can be expanded into a Taylor series around $x = 0$. This is plausible since for short chains the thickness $\sim \mathcal{R}_x$ of the polymer depletion layer is much smaller than the particle radius R so that a small curvature expansion is applicable to $f_K^{(1)}$ in which a volume term $\sim R^d$ is followed by a surface term $\sim R^{d-1}$ and by successive terms $\sim R^{d-2}$, R^{d-3}, etc., generated by the surface curvature. We note, however, that it can be rather difficult to actually prove this assumption.

The first Taylor coefficients of the expansion of $Y_{d,D}(x)$ around $x = 0$ also determine the curvature energies of a particle $\mathcal{K}$ of *more general shape* provided its surface S is smooth and all principal radii of curvature are much larger than the polymer size $\mathcal{R}_x$ (compare Ref. [25] and I). Consider the increase $F_{\mathcal{K}}$ in configurational free energy upon immersing a particle $\mathcal{K}$ with finite volume $v_{\mathcal{K}}$ into the dilute polymer solution with bulk pressure $n_p k_B T$. Due to general arguments [26] in three dimensions one expects an expansion of the Helfrich-type [27]

$$F_{\mathcal{K}} - n_p k_B T v_{\mathcal{K}} = \int_S dS \{\Delta\sigma + \Delta\kappa_1 K_m + \Delta\kappa_2 K_m^2 + \Delta\kappa_G K_G$$

$$+ \cdots\} \qquad (1.7a)$$

with the local mean curvature

$$K_m = \frac{1}{2}\left(\frac{1}{R_1} + \frac{1}{R_2}\right) \qquad (1.7b)$$

and the local Gaussian curvature

$$K_G = 1/(R_1 R_2), \qquad (1.7c)$$

where R_1 and R_2 are the two principal local radii of curvature. We use the convention that $R_1, R_2 > 0$ means that the boundary surface is bent *away* from the polymer solution located in the exterior of $\mathcal{K}$. Provided that the expansion (1.7a) is valid, the surface tension $\Delta\sigma$ and the curvature energies $\Delta\kappa_1$, $\Delta\kappa_2$, and $\Delta\kappa_G$ are determined uniquely by the special cases that $\mathcal{K}$ is a sphere and a cylinder, respectively. Our explicit results for $Y_{d,D}(x)$ provide a strong indication that the Helfrich-type expansion (1.7) is indeed valid and, moreover, does yield quantitative estimates of the surface tension and of the curvature energies for the polymer depletion problem in the presence of EV interaction. These
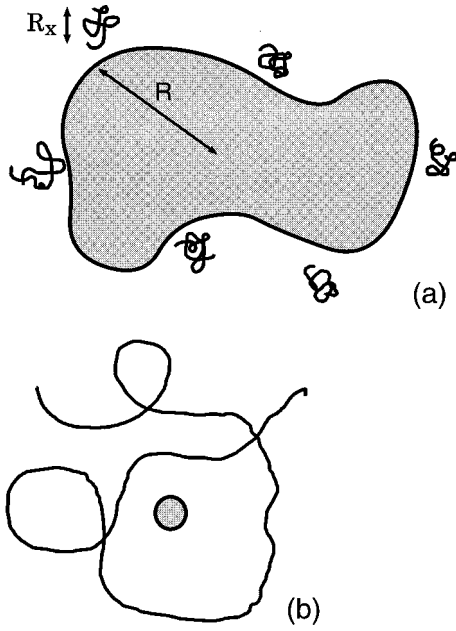
FIG. 1. Situations of short and long chains in which the limiting behavior of the scaling function $Y_{d,D}(\mathcal{R}_x/R)$ can be applied: (a) For $\mathcal{R}_x \ll R$ the function $Y_{d,D}$ determines the change of the surface tension $\Delta\sigma$ and curvature energies $\Delta\kappa_1$, $\Delta\kappa_2$, and $\Delta\kappa_G$ in the Helfrich-type expansion (1.7) of a membrane upon exposing one side of it to a dilute polymer solution. (b) For $\mathcal{R}_x \gg R$ the polymer can deform in order to avoid the space occupied by the particle and coil around a spherical (or rodlike) particle and the function $Y_{d,D}$ exhibits the power law (1.8) with the Flory exponent ν.

values are the extra contributions (as indicated by the Δ's) to the solvation free energy of a particle in addition to its background value for the polymer free solvent (i.e., $n_p = 0$), not included in Eq. (1.7a). To the best of our knowledge, this is the first check of the expansion (1.7) for a nontrivial interacting system that can be realized in nature.

For other types of systems the expansion (1.7) can be violated. For example, as pointed out by Yaman *et al.* [28], a somewhat counterintuitive behavior arises for the case in which a surface is exposed on one side to a dilute solution of thin *rigid rods* (needles): even for arbitrarily small surface curvature the free energy in this case cannot be expanded in the analytical and local form of the Helfrich-type expansion (1.7). However, for flexible ideal chains instead of needles the expansion is known to apply (see I). In particular, the asymmetry in the curvature contribution $\sim R^{-2}$ between the inside and outside of a spherical or cylindrical surface as reported by the above authors for needles does not occur for flexible ideal chains.

We note that the curvature energies are experimentally accessible. For example, the expansion (1.7) determines the change in surface tension and in the first- and second-order curvature energies of a *flexible* surface such as a *membrane* upon exposing one side of it to a solution of polymers which are depleted near the membrane [see Fig. 1(a)]. Thus the addition of polymers to a solution of closed membranes, i.e., vesicles, should influence the phase diagram of vesicle shapes in a quantitatively controllable way (see, e.g., Ref. [29]). An additional experimental access to the solvation free energy will be discussed at the end of this subsection.

(b) For *long* chains, i.e., $x \gg 1$, a single chain can deform in order to avoid the space occupied by the particle and coil around a spherical or rodlike particle [see Fig. 1(b)]. In this case it turns out that $Y_{d,D}(x)$ exhibits a power law

$$Y_{d,D}(x \to \infty) \to A_{d,D} x^{1/\nu} \tag{1.8}$$

with a dimensionless and universal amplitude $A_{d,D}$, provided

$$d > 1/\nu, \tag{1.9}$$

so that $f_K^{(1)}$ vanishes for $R \to 0$ [see Eq. (1.5)]. Here ν is the Flory exponent characterizing the power-law dependence $\mathcal{R}_x \sim N^\nu$ of $\mathcal{R}_x$ on the number N of monomers per chain if N is large. The properties described by Eqs. (1.8) and (1.9) follow from a small radius operator expansion (SRE) (see Sec. I B below).

Finally, we emphasize that $f_K^{(1)}$ is experimentally accessible by monitoring the dependence of the number density n_c of the colloidal particles on the number density n_p of the polymers in a sufficiently dilute solute of immersed particles which is in thermal equilibrium with a surrounding ideal gas phase with given partial pressure $p_c^{(0)}$ of the particles [30]. Accordingly n_c is determined by a Henry-type law

$$n_c = \frac{p_c^{(0)}}{k_B T} \Lambda^{-1}, \tag{1.10a}$$

where Λ measures the change of the solubility of the colloidal particles due to the presence of the polymers and is given by

$$\Lambda = \exp(n_p f_K^{(1)} l^\delta). \tag{1.10b}$$

For the dilute immersed particles the reduced free energy increase $n_p f_K^{(1)} l^\delta$ constitutes a reduced one-particle potential or, equivalently, an increase in chemical potential, so that Eq. (1.10) follows upon equating the chemical potentials of the particles in the ideal gas phase and in the solution phase.

B. Colloidal particles with small radii

We consider the case in which a polymer chain interacts with a spherical or cylindrical particle whose radius R—albeit being large on the microscopic scale—is much smaller than the size $\mathcal{R}_x$ of the chain and other characteristic lengths [31]. In this limiting case the effect of the spherical particle upon the configurations of the chain can be represented by a δ-function potential located at the center of the particle which repels the monomers of the chain. For a generalized cylinder K with a small radius R this δ-function potential is smeared out over its axis. Thus the Boltzmann weight $W_K\{\mathbf{y}_i\}$ for the chain [32] arising from the presence of K (whose axis includes the origin) is replaced by

$$W_K\{\mathbf{y}_i\} \to 1 - A_{d,D} R^{d-1/\nu} w_K \tag{1.11}$$

with

$$w_K = \begin{cases} \int_{\mathbb{R}^\delta} d^\delta r_\| \rho(\mathbf{r}_\perp = 0, \mathbf{r}_\|), & d < D \\ \rho(0), & d = D, \end{cases} \quad (1.12)$$

provided $d > 1/\nu$. The positions $\{\mathbf{y}_i; i = 1, \ldots, N\}$ of the N chain monomers that define the chain configuration appear in Eq. (1.12) in terms of the modified monomer density

$$\rho(\mathbf{r}) = \frac{\mathcal{R}_x^{1/\nu}}{N} \sum_{i=1}^{N} \delta^{(D)}(\mathbf{y}_i - \mathbf{r}). \quad (1.13)$$

The sum of δ functions in Eq. (1.13) is the usual monomer number density at a point $\mathbf{r}$. We have chosen its prefactor such that $\rho(\mathbf{r})$ is less dependent on the microscopic monomer structure (i.e., on what is considered as a monomer) than the sum itself. In particular, $\int d^D r \rho(\mathbf{r}) = \mathcal{R}_x^{1/\nu}$ is independent of these details while N is not. The scaling dimension $D - 1/\nu$ of $\rho(\mathbf{r})$ equals its naive inverse length dimension so that the exponent of R in Eq. (1.11) follows by comparing naive dimensions. The amplitude $A_{d,D}$ is dimensionless and universal [33].

The monomer positions $\{\mathbf{y}_i\}$ are statistical variables so that Eq. (1.11) is a relation between fluctuating quantities which is to be used inside polymer conformation averages such as the ratio of polymer partition functions with and without the presence of K. One can use Eq. (1.11) for a variety of different situations. If K is the only particle within reach of the polymer chain, Eq. (1.11) leads to the free energy change given by Eq. (1.5) in the limit discussed in Eq. (1.8). This is the reason why the same amplitude $A_{d,D}$ appears in Eqs. (1.8) and (1.11). If there are in addition other particles or walls K', Eq. (1.11) can be used to calculate the polymer-mediated free energy of interaction (potential of mean force) between K' and K (compare I and Sec. I C below). Equation (1.11) simplifies the theoretical treatment of these problems significantly because K is replaced by the monomer density $\rho(\mathbf{r})$. While the remaining, simpler averages depend on the particular problem under consideration, the universal amplitude $A_{d,D}$ is always the same.

In this work we study the small radius expansion (1.11) for the generalized cylinder K for the case of polymers in a good solvent. Our main objective is to present quantitative estimates for the universal amplitudes $A_{3,3}$ and $A_{2,3}$ corresponding to a sphere and to an infinitely elongated cylinder in three dimensions. The cylinder (i.e., $d = 2$) is particularly interesting since in this case the EV interaction changes the behavior *qualitatively*: while for ideal chains a thin cylinder is a marginal perturbation which can lead to a logarithmic behavior [10] and for which Eq. (1.11) does *not* apply, for chains with EV interaction the power-law exponent $d - 1/\nu \approx 0.30$ is *positive* and Eq. (1.11) holds. This peculiarity for $d = 2$ is reflected in the ε expansion of $A_{d,D}$ for $D = 4 - \varepsilon$.

C. Interactions between particles

Polymer-mediated interactions between particles are in general *not pairwise additive*, i.e., they cannot be written as a superposition of pair interactions [1,12]. For a dilute polymer solution with polymer density n_p we consider the total increase in reduced configurational free energy $n_p f_{\text{tot}}^{(M)}$ upon immersing spherical particles $K_1, \ldots, K_M$ centered at $\mathbf{r}_1, \ldots, \mathbf{r}_M$. The quantity $f_{\text{tot}}^{(M)}$ has the form

$$f_{\text{tot}}^{(M)}(\mathbf{r}_1, \ldots, \mathbf{r}_M) = \sum_{i=1}^{M} f_{K_i}^{(1)} + \sum_{\substack{\text{pairs} \\ i < j}}^{M} f_{K_i, K_j}^{(2)}(\mathbf{r}_i, \mathbf{r}_j) + \cdots$$

$$+ f_{K_1, \ldots, K_M}^{(M)}(\mathbf{r}_1, \ldots, \mathbf{r}_M). \quad (1.14)$$

The m-body contributions $f^{(m)}$ for $2 \le m \le M$ on the right-hand side of Eq. (1.14) are defined inductively by considering first two particles in order to define $f^{(2)}$ via Eq. (1.14), then three, and so on. For spherical particles the dimension of $f^{(m)}$ is that of a volume, i.e., of (length)^D. The existence of polymer-mediated nonpairwise interactions has first been noticed within the PHS approximation, which consists in replacing the polymer by a hard sphere [5]. Here we consider the limit for which the polymer is flexible and much longer than the particle radii, i.e., $\mathcal{R}_x \gg R$, and where the small-radius expansion (1.11) gives a simple and *quantitative* description. We find that the polymer-mediated interaction for particles with small R is *drastically* different from the depletion interaction for large R in which case the PHS approximation is reasonable and has been widely used. This confirms the generally accepted belief that for the applicability of the PHS approximation a large size ratio $R/\mathcal{R}_x$ is crucial and refutes an opposite claim in Ref. [9](b).

As illustration we consider three spherical particles A, B, C with radii R_A, R_B, R_C much smaller than their mutual distances and than $\mathcal{R}_x$. It is easy to see that $f_{\text{tot}}^{(3)}$ is determined by the Boltzmann weights of the particles introduced in the text preceding Eq. (1.11) in the form

$$f_{\text{tot}}^{(3)}(\mathbf{r}_A, \mathbf{r}_B, \mathbf{r}_C) = \int_{\mathbb{R}^D} d^D y \{1 - W_A W_B W_C\}_\mathbf{y}, \quad (1.15)$$

where $\{\}_\mathbf{y}$ denotes the average over all conformations of a single chain in *free* space (i.e., no particles) under the constraint that one end of the chain is fixed at the point $\mathbf{y}$. In the limit of small radii R one finds by using Eq. (1.11) that in addition to the one-body contributions $f_A^{(1)}$, $f_B^{(1)}$, and $f_C^{(1)}$, each exhibiting the scaling form described by Eq. (1.5) in the limit given by Eq. (1.8), there arise two-body contributions

$$f_{A,B}^{(2)} \rightarrow -(A_{D,D})^2 (R_A R_B)^{D - 1/\nu} C_2(\mathbf{r}_A, \mathbf{r}_B), \quad (1.16a)$$

$f_{A,C}^{(2)}$, and $f_{B,C}^{(2)}$, and a three-body contribution

$$f_{A,B,C}^{(3)} \rightarrow (A_{D,D})^3 (R_A R_B R_C)^{D - 1/\nu} C_3(\mathbf{r}_A, \mathbf{r}_B, \mathbf{r}_C). \quad (1.16b)$$

The arrows in the above relations indicate the leading behavior for small radii. Here C_2 and C_3 are pair and triple correlation functions corresponding to

$$C_m(\mathbf{r}_1, \mathbf{r}_2, \ldots, \mathbf{r}_m) = \int_{\mathbb{R}^D} d^D y \{\rho(\mathbf{r}_1) \rho(\mathbf{r}_2) \cdots \rho(\mathbf{r}_m)\}_\mathbf{y} \quad (1.17)$$

of the (modified) monomer density $\rho(\mathbf{r})$ defined in Eq. (1.13) for a single polymer chain in free space. Since $\mathcal{R}_x$ and the relative distances $r_{AB} = |\mathbf{r}_A - \mathbf{r}_B|$ are large on the microscopic scale, these correlation functions exhibit the scaling forms

$$C_2(\mathbf{r}_A, \mathbf{r}_B) = \mathcal{R}_x^{2/\nu - D} g(z_{AB}), \qquad (1.18a)$$

with $z_{AB} = r_{AB}/\mathcal{R}_x$, and

$$C_3(\mathbf{r}_A, \mathbf{r}_B, \mathbf{r}_C) = \mathcal{R}_x^{3/\nu - 2D} h(z_{AB}, z_{AC}, z_{BC}), \quad (1.18b)$$

which follow from the scaling dimension $D - 1/\nu$ of $\rho(\mathbf{r})$. Thus for three spherical particles with equal radii R and with center-to-center distances r_{AB}, r_{AC}, r_{BC} which are of the order of $\mathcal{R}_x$ but much larger than R, the three-body interaction is smaller than the two-body interaction by a factor $\sim (R/\mathcal{R}_x)^{D - 1/\nu}$.

Similar fluctuation-induced, non-pairwise-additive interactions arise between particles which are immersed in a near-critical fluid mixture [34]. In this case one encounters order parameter correlation functions instead of the present monomer density correlation functions.

The small radius expressions (1.16) cease to apply—even if the equal radii R are much smaller than $\mathcal{R}_x$—if some of the relative distances between the spheres become comparable with R. However, there are other types of short distance expansions which are capable of describing these latter situations. In particular we shall discuss a ''small dumbbell'' expansion for a pair of spheres A, B for which both R and r_{AB} are much smaller than the other lengths. The structure of this expansion is similar to Eq. (1.11) in conjunction with the lower part of Eq. (1.12), but the amplitude corresponding to $A_{D,D}$ now depends on the ratio r_{AB}/R. We calculate this new amplitude function for the case of ideal chains.

In Sec. II we discuss in detail the solvation free energy for a single particle. In Sec. III we consider the depletion interaction between particles. Section IV contains our conclusions. In Appendix A we derive the asymptotic expansions for a small and large size ratio $\mathcal{R}_x/R$ required for Sec. II. In Appendix B we discuss the perturbative treatment of the small radius operator expansion. Finally, in Appendix C, we derive a short-distance amplitude which characterizes the behavior of monomer density correlation functions in free space as needed in Sec. III.

II. SOLVATION FREE ENERGY OF A PARTICLE

The free energy for immersing a particle in a dilute solution of freely floating chains with or without self-avoidance can be expressed in terms of the density profile of chain ends in the presence of the particle [compare, e.g., Eq. (3.7) in I]. For the scaling function introduced in Eq. (1.5) this implies

$$Y_{d,D}(x) = \frac{\Omega_d}{d} + \Omega_d Q_{d,D}(\eta), \qquad \eta = x^2/2, \qquad (2.1)$$

with $\Omega_d = 2\pi^{d/2}/\Gamma(d/2)$, the surface area of the d-dimensional unit sphere, and

$$Q_{d,D}(\eta) = \int_1^\infty d\rho \, \rho^{d-1} [1 - M_E(\rho, \eta)]. \qquad (2.2)$$

In Eq. (2.2) the scaling function $M_E(r_\perp/R, \eta)$ is the bulk normalized density profile of chain ends at a distance $r_\perp - R$ from the particle surface. In Sec. II A we derive the explicit form of $Q_{d,D}(\eta)$ in the presence of EV interaction to lowest nontrivial order in $\varepsilon = 4 - D$. In Secs. II B and II C we

discuss the resulting behavior of $Y_{d,D}(x)$ in the limit of short and long chains, respectively. Finally, we obtain in Sec. II D an approximation for the full scaling function $Y_{3,3}(x)$ corresponding to a sphere in $D = 3$.

A. Density of chain ends and polymer magnet analogy

We employ the polymer magnet analogy (PMA) in order to calculate the density profile $\mathcal{M}_E$ of chain ends in a dilute solution of chains with EV interaction which arises in the presence of the nonadsorbing generalized cylinder K introduced in Eq. (1.3). As in I we define $\mathcal{M}_E$ as bulk normalized so that it approaches 1 far from the particle. It is given by

$$\mathcal{M}_E(r_\perp; L_0, R, u_0)$$
$$= \int_V d^D r' Z(\mathbf{r}, \mathbf{r}'; L_0, R, u_0) \bigg/ \int_V d^D r' Z_b(\mathbf{r}, \mathbf{r}'; L_0, u_0).$$
$$(2.3)$$

Here Z and Z_b are partition functions of a single chain with the two ends fixed at $\mathbf{r}$, $\mathbf{r}'$ in the presence and absence, respectively, of the generalized cylinder K (the subscript b stands for ''bulk''). The volume V available for the chain is the outer space $V = \mathbb{R}^D \backslash K$ of K. The parameter u_0 characterizes the strength of the EV interaction and L_0 determines the monomer content or ''length'' of the chain such that $2L_0$ equals the mean square $\mathcal{R}_x^2$ of the projected end-to-end distance of the chain in the absence of K and of the EV interaction, i.e., for $u_0 = 0$. The usual arguments of the PMA [15,17–19] carry over to the present case and imply the correspondence

$$Z(\mathbf{r}, \mathbf{r}'; L_0, R, u_0) = \mathcal{L}_{t_0 \to L_0} \langle \Phi_1(\mathbf{r}) \Phi_1(\mathbf{r}') \rangle |_{\mathcal{N}=0} \quad (2.4)$$

between Z and the two-point correlation function $\langle \Phi_1(\mathbf{r}) \Phi_1(\mathbf{r}') \rangle$ in an $O(\mathcal{N})$-symmetric field theory for an $\mathcal{N}$-component order parameter field $\mathbf{\Phi} = (\Phi_1, \ldots, \Phi_{\mathcal{N}})$ in the restricted volume $V = \mathbb{R}^D \backslash K$. In Eq. (2.4) the operation

$$\mathcal{L}_{t_0 \to L_0} = \frac{1}{2\pi i} \int_{\mathcal{C}} dt_0 e^{L_0 t_0} \qquad (2.5)$$

acting on the correlation function is an inverse Laplace transform with $\mathcal{C}$ a path in the complex t_0 plane to the right of all singularities of the integrand. The Laplace conjugate t_0 of L_0 and the excluded volume strength u_0 appear, respectively, as the temperature parameter and the prefactor of the $(\mathbf{\Phi}^2)^2$ term in the Ginzburg-Landau Hamiltonian

$$\mathcal{H}_K\{\mathbf{\Phi}\} = \int_V d^D r \left\{ \frac{1}{2}(\nabla\mathbf{\Phi})^2 + \frac{t_0}{2}\mathbf{\Phi}^2 + \frac{u_0}{24}(\mathbf{\Phi}^2)^2 \right\},$$
$$(2.6a)$$

which provides the statistical weight $\exp(-\mathcal{H}_K\{\mathbf{\Phi}\})$ for the field theory. The position vector $\mathbf{r}$ covers the volume V and its boundary, which is the surface of K. In order to be consistent with Eq. (1.1) we have to impose the Dirichlet condition

$$\mathbf{\Phi}(\mathbf{r}) = \mathbf{0} \quad \text{if} \quad |\mathbf{r}_\perp| = R \qquad (2.6b)$$

on the boundary. This corresponds to the fixed point bound-

ary condition of the so-called ordinary transition [35,36] for the field theory. For our renormalization-group improved perturbative investigations we use a dimensionally regularized continuum version of the field theory which we shall renormalize by minimal subtraction of poles in $\varepsilon = 4 - D$

$$\langle \Phi_i(\mathbf{r})\Phi_j(\mathbf{r}')\rangle_{[0]} = \delta_{ij}G(\mathbf{r},\mathbf{r}';t_0,R) = \delta_{ij}\hat{G}(r_\perp,r_\perp',\vartheta,|\mathbf{r}_\parallel-\mathbf{r}_\parallel'|;t_0,R)$$

$$= \delta_{ij} \times \begin{cases} \sum_{n=0}^\infty W_n^{(\alpha)}(\vartheta)\int_{\mathbb{R}^\delta}\frac{d^\delta P}{(2\pi)^\delta}\exp[i\mathbf{P}(\mathbf{r}_\parallel-\mathbf{r}_\parallel')]\widetilde{G}_n(r_\perp,r_\perp';\mathcal{S},R), & d<D \\ \sum_{n=0}^\infty W_n^{(\alpha)}(\vartheta)\widetilde{G}_n(r_\perp,r_\perp';t_0,R), & d=D, \end{cases} \tag{2.7a}$$

where $\alpha = (d-2)/2$, $\mathcal{S} = P^2 + t_0$, $r_\perp = |\mathbf{r}_\perp|$, and ϑ is the angle between $\mathbf{r}_\perp$ and $\mathbf{r}_\perp'$ (compare Fig. 1 in I). Note that for $d=D$ [last line in Eq. (2.7a)] there is no parallel component $\mathbf{r}_\parallel-\mathbf{r}_\parallel'$ and hence no Fourier variable $\mathbf{P}$. The functions $W_n^{(\alpha)}(\vartheta)$ are given by

$$W_n^{(\alpha)}(\vartheta) = \begin{cases} (2\pi^{d/2})^{-1}\Gamma(\alpha)(n+\alpha)C_n^\alpha(\cos\vartheta), & d\neq 2 \\ (2\pi)^{-1}(2-\delta_{n,0})\cos(n\vartheta), & d=2, \end{cases} \tag{2.7b}$$

where Γ is the gamma function, C_n^α are Gegenbauer polynomials [38], and $\delta_{n,0}=1$ for $n=0$ and zero otherwise. The functions $W_n^{(\alpha)}$ are normalized so that $\int d\Omega_d W_n^{(\alpha)} = \delta_{n,0}$. The propagator $\widetilde{G}_n$ has the form

$$\widetilde{G}_n(r_\perp,r_\perp';\mathcal{S},R) = (r_\perp^{(<)}r_\perp^{(>)})^{-\alpha}K_{\alpha+n}(\sqrt{\mathcal{S}}r_\perp^{(>)})$$

$$\times\left[I_{\alpha+n}(\sqrt{\mathcal{S}}r_\perp^{(<)})\right.$$

$$\left. -\frac{I_{\alpha+n}(\sqrt{\mathcal{S}}R)}{K_{\alpha+n}(\sqrt{\mathcal{S}}R)}K_{\alpha+n}(\sqrt{\mathcal{S}}r_\perp^{(<)})\right], \tag{2.7c}$$

where $r_\perp^{(<)} = \min(r_\perp,r_\perp')$ and $r_\perp^{(>)} = \max(r_\perp,r_\perp')$. For $d=D$ the variable $\mathcal{S}$ is replaced by t_0. I_α and K_α denote modified Bessel functions [38].

The numerator in the density profile $\mathcal{M}_E$ in Eq. (2.3) can be obtained from the integrated two-point correlation function, i.e., the local susceptibility χ, for $t_0>0$. Due to rotational invariance around and translational invariance along the axis of K, the local susceptibility χ only depends on the radial component $r_\perp$ of the point $\mathbf{r}=(\mathbf{r}_\perp,\mathbf{r}_\parallel)$. The loop expansion of χ reads

$$\chi(r_\perp;t_0,R,u_0) = \chi^{[0]}(r_\perp;t_0,R) + u_0\chi^{[1]}(r_\perp;t_0,R) + O(u_0^2), \tag{2.8}$$

where the zero-loop contribution $\chi^{[0]}$ is given by the integrated propagator

[37] [this is related via Eq. (2.4) to a corresponding procedure in the Edwards model [17–19]]. The basic element of the perturbation expansion is the Gaussian two-point correlation function (or propagator) $\langle\Phi_i(\mathbf{r})\Phi_j(\mathbf{r}')\rangle_{[0]}$ where the subscript [0] denotes $u_0=0$. It is given by

$$\chi^{[0]}(r_\perp;t_0,R) = \int_V d^D r'\, G(\mathbf{r},\mathbf{r}';t_0,R)$$

$$= \frac{R^2}{\tau_0}\left[1 - \frac{\rho^{-\alpha}K_\alpha(\rho\sqrt{\tau_0})}{K_\alpha(\sqrt{\tau_0})}\right]. \tag{2.9}$$

The greek symbols on the right-hand side (rhs) denote dimensionless variables expressed in terms of the radius R of K:

$$\tau_0 = t_0 R^2, \quad \rho = r_\perp/R. \tag{2.10}$$

According to standard perturbation theory the one-loop contribution is given by

$$u_0\chi^{[1]}(r_\perp;t_0,R) = -\frac{\mathcal{N}+2}{3}\frac{u_0}{2}\int_V d^D y\, G(\mathbf{r},\mathbf{y};t_0,R)$$

$$\times G(\mathbf{y},\mathbf{y};t_0,R)\chi^{[0]}(y_\perp;t_0,R)$$

$$= -\frac{\mathcal{N}+2}{3}\frac{u_0}{2}R^{2+\varepsilon}\int_1^\infty d\psi\,\psi^{\varepsilon-1}\mathcal{G}(\rho,\psi,\tau_0)$$

$$\times g(\psi,\tau_0,\varepsilon)\mathcal{X}^{[0]}(\psi,\tau_0), \tag{2.11}$$

where $\psi = y_\perp/R$ [compare Eq. (2.10)]. The functions in the integrand of the last line in Eq. (2.11) are dimensionless and defined by

$$\mathcal{X}^{[0]}(\psi,\tau_0) = R^{-2}\chi^{[0]}(y_\perp;t_0,R), \tag{2.12}$$

$$\mathcal{G}(\rho,\psi,\tau_0) = R^{2\alpha}\widetilde{G}_{n=0}(r_\perp,y_\perp;\mathcal{S}=t_0,R), \tag{2.13}$$

$$y_\perp^\varepsilon g(\psi,\tau_0,\varepsilon) = y_\perp^d R^{-2\alpha}G(\mathbf{y},\mathbf{y};t_0,R). \tag{2.14}$$

The function g can be split into $g=g_b+g_s$, where

$$g_b(\psi,\tau_0,\varepsilon) = \tau_0^{1-\varepsilon/2}\psi^{d-\varepsilon}\frac{\Gamma(\varepsilon/2-1)}{(4\pi)^{D/2}} \tag{2.15a}$$

stems from the bulk contribution of $G(\mathbf{y},\mathbf{y};t_0,R)$ and

$$g_s(\psi,\tau_0,\varepsilon) = -\psi^{2-\varepsilon}\sum_{n=0}^{\infty}W_n^{(\alpha)}(\vartheta=0)\begin{cases}\dfrac{\Omega_\delta}{(2\pi)^\delta}\displaystyle\int_0^\infty dq\,q^{\delta-1}\dfrac{I_{\alpha+n}(\sqrt{q^2+\tau_0})}{K_{\alpha+n}(\sqrt{q^2+\tau_0})}[K_{\alpha+n}(\psi\sqrt{q^2+\tau_0})]^2, & d<D\\[4mm] \dfrac{I_{\alpha+n}(\sqrt{\tau_0})}{K_{\alpha+n}(\sqrt{\tau_0})}[K_{\alpha+n}(\psi\sqrt{\tau_0})]^2, & d=D.\end{cases} \tag{2.15b}$$

Note that $\delta=D-d=4-\varepsilon-d$. In the case $d<D$ we shall consider d [and $\alpha=(d-2)/2$] as a variable which is *independent* of $D=4-\varepsilon$ whereas in the case $d=D$ the variable $\alpha=1-\varepsilon/2$ depends of course on ε. One can check that in the case $d=1$, for which $W_n^{(\alpha)}(\vartheta=0)$ with $\alpha=-1/2$ contributes only for $n=0$ and 1, the upper part of Eq. (2.15b) leads indeed to the half-space result

$$G(\mathbf{y},\mathbf{y};t_0,R)-G_b(\mathbf{y},\mathbf{y};t_0) = -\frac{\Omega_{D-1}}{(2\pi)^{D-1}}\int_0^\infty dP\,\frac{P^{D-2}}{2\sqrt{P^2+t_0}}\exp[-2\sqrt{P^2+t_0}(y_\perp-R)], \quad d=1, \tag{2.15c}$$

where the integral can be expressed in terms of a modified Bessel function. We add the following two remarks about the behavior of g_s for $d>1$ if $R\to\infty$ or $R\to0$.

(i) It is instructive to see how the behavior for the half-space arises by taking the limit $R\to\infty$ with t_0 and $y_\perp-R$ fixed. Consider, e.g., the case $d=D=4$ corresponding to the sphere in four dimensions. Since upon approaching the above limit the arguments of the Bessel functions in the lower Eq. (2.15b) become large and since many terms contribute in the sum over n, one has to use the uniform asymptotic expansion of the Bessel functions [compare, e.g., Eqs. 9.7.7 and 9.7.8 in Ref. [38(a)]] and may replace the sum by an integral. This yields that $G(\mathbf{y},\mathbf{y};t_0,R)-G_b(\mathbf{y},\mathbf{y};t_0)$ for $d=D=4$ does indeed tend to the half-space expression on the rhs of Eq. (2.15c) with $D=4$, where the role of the length P of the wave vector $\mathbf{P}$ is taken by the ratio n/R.

(ii) For $d>2$ and fixed nonvanishing lengths $y_\perp$ and $t_0^{-1/2}$ the quantity $g_s(\psi,\tau_0,\varepsilon)$ has a finite limit for $R\to0$, i.e.,

$$g_s^{(\mathrm{as})}(\psi\sqrt{\tau_0},\varepsilon)\equiv\lim_{R\to0}g_s(\psi,\tau_0,\varepsilon) = -\frac{2^{2-d}}{\pi^{d/2}\Gamma(\alpha)}\begin{cases}\dfrac{\Omega_\delta}{(2\pi)^\delta}\displaystyle\int_0^\infty dk\,k^{\delta-1}(k^2+\psi^2\tau_0)^\alpha[K_\alpha(\sqrt{k^2+\psi^2\tau_0})]^2, & d<D\\[4mm] (\psi^2\tau_0)^\alpha[K_\alpha(\psi\sqrt{\tau_0})]^2, & d=D,\end{cases} \tag{2.15d}$$

which depends only on the R-independent product $\psi\sqrt{\tau_0}$ $=y_\perp\sqrt{t_0}$ and describes the behavior of g_s for $R\ll y_\perp$, $t_0^{-1/2}$. This is consistent with the operator expansion for small radius R of the Boltzmann weight representing K when applied to a Gaussian field theory (compare I). While $g_s^{(\mathrm{as})}$ decays exponentially for $\psi\sqrt{\tau_0}\to\infty$, it approaches a finite constant for $\psi\sqrt{\tau_0}\to0$, which equals $-\alpha/(4\pi^2)$ for $\varepsilon=0$ and characterizes the behavior of g_s for $R\ll y_\perp\ll t_0^{-1/2}$. This should be compared with the behavior $g_s\sim-(\psi-1)^{2-D}$ which applies *close to the surface* of K, i.e., for $0<y_\perp-R\ll R$, $t_0^{-1/2}$.

The reparametrizations [37]

$$u_0=16\pi^2 f(\epsilon)\mu^\varepsilon Z_u u, \quad Z_u=1+O(u), \tag{2.16a}$$

and

$$t_0=\mu^2 Z_t t=\mu^2\left(1+\frac{\mathcal{N}+2}{3}\frac{u}{\varepsilon}+O(u^2)\right)t \tag{2.16b}$$

of the bare bulk parameters u_0 and t_0 in terms of their renormalized and dimensionless counterparts u and t are not affected by the presence of the surface [39,36]. Here μ is the inverse length scale which determines the renormalization-group flow and $f(\varepsilon)=1+\varepsilon f_1+O(\varepsilon^2)$. The coefficient f_1 drops out from universal quantities and therefore can be chosen arbitrarily. Equation (2.16b) implies the renormalized counterpart

$$\tau=(\mu R)^2 t \tag{2.16c}$$

of τ_0. The renormalized, i.e., pole-free, local susceptibility χ_{ren} is related to χ by [36,37]

$$\chi_{\mathrm{ren}}(r_\perp;t,R,u)=\chi(r_\perp;t_0,R,u_0)/Z_\Phi(u)$$
$$=\chi(r_\perp;t_0,R,u_0)+O(u^2) \tag{2.16d}$$

with the renormalization factor Z_Φ of the field Φ which deviates from one only in second order in u. The only pole in $\chi^{[1]}$ is due to the bulk contribution g_b in Eq. (2.15a). When the results for $\chi^{[0]}$ and $u_0\chi^{[1]}$ in Eqs. (2.9) and (2.11) are substituted into Eq. (2.8) and when the bare parameters τ_0 and u_0 are expressed in terms of their renormalized counterparts τ and u according to Eqs. (2.16), the poles in ε cancel indeed [39]. This cancellation can be traced back to the relation

$$\int_1^\infty d\psi\,\psi^{d-1}\mathcal{G}(\rho,\psi,\tau)\mathcal{X}^{[0]}(\psi,\tau)=-\frac{\partial}{\partial\tau}\mathcal{X}^{[0]}(\rho,\tau). \tag{2.17}$$

The resulting renormalized and scaled local susceptibility $\mathcal{X}_{\mathrm{ren}}=R^{-2}\chi_{\mathrm{ren}}$ up to one-loop order reads

$$\mathcal{X}_{\text{ren}}(\rho,\tau,\mu R,u) = \mathcal{X}^{[0]}(\rho,\tau) + \frac{\mathcal{N}+2}{3}u$$

$$\times\left[\left(\frac{\ln\tau}{2} - \ln(\mu R) + B\right)\tau\frac{\partial}{\partial\tau}\mathcal{X}^{[0]}(\rho,\tau)\right.$$

$$\left. + \mathcal{E}_d(\rho,\tau)\right] + O(u^2) \qquad (2.18)$$

with the nonuniversal constant

$$B = \frac{C_E}{2} - \frac{1}{2} - f_1 - \frac{\ln(4\pi)}{2}, \qquad (2.19)$$

where C_E is Euler's constant, and the function

$$\mathcal{E}_d(\rho,\tau) = -8\pi^2\int_1^\infty d\psi\,\psi^{-1}\mathcal{G}(\rho,\psi,\tau)$$

$$\times g_s(\psi,\tau,\varepsilon=0)\mathcal{X}^{[0]}(\psi,\tau). \qquad (2.20)$$

Since $\mathcal{E}_d$ belongs to the one loop contribution and because in the last line of Eq. (2.11) the order of the ψ integration and the limit $\varepsilon\to 0$ can be interchanged, we set $\varepsilon=0$ in the integrand on the rhs of Eq. (2.20). This implies that in the case $d=D$ only $\mathcal{E}_4$ enters into Eq. (2.18) [compare the remark below Eq. (2.15b)]. The integral on the rhs of Eq. (2.20) is well-defined since the divergence of $g_s(\psi,\tau,\varepsilon=0)$ for $\psi\searrow 1$ becomes integrable due to the Dirichlet behavior of $\mathcal{G}$ and $\mathcal{X}^{[0]}$ as implied by Eq. (2.6b). We also need the bulk value (far away from K) of the renormalized local susceptibility up to one-loop order, which reads

$$\mathcal{X}_{\text{ren},b}(\tau,\mu R,u) = \frac{1}{\tau} - \frac{\mathcal{N}+2}{3}\frac{u}{\tau}\left(\frac{\ln\tau}{2} - \ln(\mu R) + B\right)$$

$$+ O(u^2). \qquad (2.21)$$

The perturbative result (2.18) can be improved using standard renormalization-group arguments [36]. Although we need only the results (2.18) and (2.21) for the discussion of the polymer-depletion problem, we note that in the asymptotic limit for which $r_\perp$, R, and the bulk correlation length ξ_+ for $t>0$ are large compared with microscopic lengths, the ratio

$$\mathcal{X}_{\text{ren}}(\rho,\tau,\mu R,u)/\mathcal{X}_{\text{ren},b}(\tau,\mu R,u) \to \Xi_{\mathcal{N}}(\rho,\gamma) \quad (2.22)$$

yields a scaling form expressed in terms of the universal scaling function $\Xi_{\mathcal{N}}(\rho,\gamma)$ with the scaling variables $\rho = r_\perp/R$ and $\gamma = R^2/\xi_+^2$. The function $\Xi_{\mathcal{N}}$ depends on the number $\mathcal{N}$ of components of $\mathbf{\Phi}$, on the parameter d, which characterizes the shape of K, and on the space dimension D. While the amplitude ξ_0^+ in the bulk relation $\xi_+ = \xi_0^+ t^{-\nu(\mathcal{N})}$ is nonuniversal, the exponent $\nu(\mathcal{N})$ is universal and depends only on $\mathcal{N}$ and D. The asymptotic scaling behavior is governed by the infrared (long-distance) stable fixed point for which

$$u = u^* = \frac{3\varepsilon}{\mathcal{N}+8} + O(\varepsilon^2) \qquad (2.23)$$

and

$$\nu(\mathcal{N}) = \frac{1}{2} + \frac{1}{4}\frac{\mathcal{N}+2}{\mathcal{N}+8}\varepsilon + O(\varepsilon^2). \qquad (2.24)$$

The bulk correlation length ξ_+ can be defined in various ways. For definiteness we assume that ξ_+^2 is defined as the second moment of the two-point correlation function divided by $2D$, which implies

$$(\xi_0^+)^2 = [D_t(u)]^{-2\nu(\mathcal{N})}\left\{\mu^{-2}\left[1 - \frac{\mathcal{N}+2}{\mathcal{N}+8}\varepsilon B + O(\varepsilon^2)\right]\right\} \qquad (2.25)$$

with the nonuniversal constant B defined in Eq. (2.19). Here the curly bracket equals ξ_+^2 for $t=1$ and $u=u^*$, and the dependence of $(\xi_0^+)^2$ on u is contained in the dimensionless amplitude D_t which can be expressed in terms of Wilson functions corresponding to the renormalization-group flow of t and u [37,17–19]. When Eqs. (2.23)–(2.25) are combined with Eqs. (2.18) and (2.21), one finds that $\mathcal{X}_{\text{ren}}/\mathcal{X}_{\text{ren},b}$ at the fixed point is indeed consistent with Eq. (2.22) and that the scaling function $\Xi_{\mathcal{N}}$ is given by

$$\Xi_{\mathcal{N}}(\rho,\gamma) = \gamma\mathcal{X}^{[0]}(\rho,\gamma) + \frac{\mathcal{N}+2}{\mathcal{N}+8}\varepsilon\,\gamma\mathcal{E}_d(\rho,\gamma) + O(\varepsilon^2). \qquad (2.26)$$

Equation (2.26) provides the general result for the bulk normalized local susceptibility of the magnetic analog in the presence of K.

The density $\mathcal{M}_E$ of chain ends as defined in Eq. (2.3) can be related to $\mathcal{X}_{\text{ren}} = R^{-2}\chi_{\text{ren}}$, with χ_{ren} from Eq. (2.16d), by means of Eqs. (2.4) and (2.16). The result is

$$\mathcal{M}_E(r_\perp;L_0,R,u_0) = \mathcal{Z}_{\text{ren}}(\rho,\lambda,\mu R,u)/\mathcal{Z}_{\text{ren},b}(\lambda,\mu R,u), \qquad (2.27a)$$

where

$$\mathcal{Z}_{\text{ren}}(\rho,\lambda,\mu R,u) = \mathcal{L}_{\tau\to\lambda}\{\mathcal{X}_{\text{ren}}(\rho,\tau,\mu R,u)\}|_{\mathcal{N}=0} \qquad (2.27b)$$

is the renormalized and scaled version of the integrated chain partition function in the numerator of the rhs of Eq. (2.3). Here $\mathcal{L}$ is the operation in Eq. (2.5) and

$$\lambda = L/(\mu R)^2 = Z_t L_0/R^2 \qquad (2.27c)$$

is the scaled counterpart of the renormalized and dimensionless chain "length" L [17–19] so that $\lambda\tau = Lt = L_0 t_0$. For large $r_\perp$, L_0, R the end density exhibits the scaling behavior

$$\mathcal{M}_E(r_\perp;L_0,R,u_0) \to M_E(\rho,\eta), \qquad (2.27d)$$

where M_E is a universal scaling function of $\rho = r_\perp/R$ and the scaling variable

$$\eta = \frac{\mathcal{R}_x^2}{2R^2}. \qquad (2.27e)$$

According to our definition in Eq. (1.2) of $\mathcal{R}_E^2 = D\mathcal{R}_x^2$ as the second moment of the bulk partition function $Z_b(\mathbf{r},\mathbf{r}')$ the

nonuniversal prefactor r_0^2 in the asymptotic behavior $\mathcal{R}_E^2/(2D) = r_0^2 L^{2\nu}$, with $\nu = \nu(\mathcal{N}=0)$, has the form

$$r_0^2 = [D_L(u)]^{2\nu} \left\{ \mu^{-2} \left[1 - \frac{\varepsilon}{4} \left(B + 1 - \frac{C_E}{2} \right) + O(\varepsilon^2) \right] \right\}$$
(2.28)

with B from Eq. (2.19). The curly bracket equals $\mathcal{R}_E^2/(2D)$ for $L=1$ and $u=u^*$ and the dependence of r_0^2 on u is contained in the amplitude $D_L = 1/D_t$, with D_t from Eq. (2.25) (compare, e.g., Ref. [19]). Obviously η plays a similar role as the inverse of the scaling variable $\gamma = R^2/\xi_+^2$ in Eq. (2.26) in the magnetic analog. By using Eqs. (2.27a) and (2.27b) and by carrying out the same steps which lead to the scaling function $\Xi_{\mathcal{N}}$ in Eq. (2.26) of the magnetic analog, one arrives at

$$M_E(\rho, \eta) = M_E^{[0]}(\rho, \eta) + \frac{\varepsilon}{4} M_E^{[1]}(\rho, \eta) + O(\varepsilon^2),$$
(2.29a)

where

$$M_E^{[0]}(\rho, \eta) = \mathcal{L}_{\tau \to \eta} \{ \mathcal{X}^{[0]}(\rho, \tau) \}$$
(2.29b)

is the zero-loop, i.e., Gaussian contribution and [40]

$$M_E^{[1]}(\rho, \eta) = \mathcal{L}_{\tau \to \eta} \{ \mathcal{E}_d(\rho, \tau) \} + \mathcal{L}_{\tau \to \eta} \left\{ \frac{\ln \tau}{2} \left[\tau \frac{\partial}{\partial \tau} \mathcal{X}^{[0]}(\rho, \tau) \right. \right.$$
$$\left. \left. + \frac{1}{\tau} \right] \right\} + \frac{1}{2} \left[1 - M_E^{[0]}(\rho, \eta) - \eta \frac{\partial}{\partial \eta} M_E^{[0]}(\rho, \eta) \right]$$
$$\times [\ln \eta + C_E] + \eta \frac{\partial}{\partial \eta} M_E^{[0]}(\rho, \eta).$$
(2.29c)

Equation (2.29) provides the general result for the bulk normalized density of chain ends M_E in a dilute polymer solution in the presence of K. According to Eq. (2.2) for the scaling function $Y_{d,D}$ we only need the integrated form. The terms in Eq. (2.29c) have been arranged such that the ρ integration in Eq. (2.2) can be carried out in each bracket separately. This leads to

$$Q_{d,D}(\eta) = P_d^{[0]}(\eta) + \frac{\varepsilon}{4} P_d^{[1]}(\eta) + O(\varepsilon^2),$$
(2.30a)

where

$$P_d^{[0]}(\eta) = \mathcal{L}_{\tau \to \eta} \left\{ \frac{K_{\alpha+1}(\sqrt{\tau})}{\tau^{3/2} K_\alpha(\sqrt{\tau})} \right\}$$
(2.30b)

is the zero-loop, i.e., Gaussian contribution and

$$P_d^{[1]}(\eta) = -C_d(\eta) + \mathcal{L}_{\tau \to \eta} \left\{ \frac{\tau \ln \tau}{2} \frac{\partial}{\partial \tau} \left[\frac{K_{\alpha+1}(\sqrt{\tau})}{\tau^{3/2} K_\alpha(\sqrt{\tau})} \right] \right\}$$
$$- \frac{1}{2} \left[P_d^{[0]}(\eta) + \eta \frac{\partial}{\partial \eta} P_d^{[0]}(\eta) \right] [\ln \eta + C_E]$$
$$+ \eta \frac{\partial}{\partial \eta} P_d^{[0]}(\eta).$$
(2.30c)

In Eq. (2.30c) we have introduced the function

$$C_d(\eta) = \mathcal{L}_{\tau \to \eta} \{ \mathcal{C}_d(\tau) \}$$
(2.31a)

with

$$\mathcal{C}_d(\tau) = \int_1^\infty d\rho \, \rho^{d-1} \mathcal{E}_d(\rho, \tau)$$
$$= -8 \pi^2 \int_1^\infty d\psi \, \psi^{-1} g_s(\psi, \tau, \varepsilon = 0)$$
$$\times [\mathcal{X}^{[0]}(\psi, \tau)]^2,$$
(2.31b)

where Eq. (2.20) has been used. The functions in the integrand of the last line in Eq. (2.31b) are given by Eqs. (2.15b) and (2.12) in conjunction with Eq. (2.9). In the case $d=D$ we have to consider $\mathcal{C}_4(\tau)$ only [compare the remark below Eq. (2.20)].

B. Short chains: $Y_{d,D}(x)$ for $x \to 0$

The aim of this subsection is to determine the surface tension $\Delta \sigma$ and the curvature energies $\Delta \kappa_1$, $\Delta \kappa_2$, and $\Delta \kappa_G$ in the expansion (1.7) to first order in $\varepsilon = 4 - D$ by considering the special cases that the particle $\mathcal{K}$ is a generalized cylinder K with $d=D$, 3, and 2.

The analyticity of $Y_{d,D}(x)$ at $x=0$ mentioned in Sec. I A is corroborated by our first-order results in Eqs. (2.30) and (2.31) for $Q_{d,D}(\eta)$, which can be expanded into a Taylor series in $\sqrt{\eta} = x/\sqrt{2}$. In the following we determine the first three terms of this expansion. The expansion is consistent with the behavior

$$\mathcal{C}_d(\tau) = \mathcal{C}_0 \tau^{-3/2} + \mathcal{C}_1^{(d)} \tau^{-2} + \mathcal{C}_2^{(d)} \tau^{-5/2} + O(\tau^{-3})$$
(2.32)

for large $\tau = (\mu R)^2 t$ of the function $\mathcal{C}_d(\tau)$ in Eq. (2.31b) which we verify in Appendix A. Its form [40]

$$Q_{d,D}(\eta) = \frac{2 \eta^{1/2}}{\sqrt{\pi}} \left\{ 1 - \frac{\varepsilon}{4} \left[1 - \frac{3 \ln 2}{2} + \mathcal{C}_0 \right] \right\}$$
$$+ \eta \left\{ \frac{d-1}{2} - \frac{\varepsilon}{4} \mathcal{C}_1^{(d)} \right\} + \frac{4 \eta^{3/2}}{3 \sqrt{\pi}} \left\{ \frac{(d-1)(d-3)}{8} \right.$$
$$\times \left[1 - \frac{\varepsilon}{4} \left(\frac{11}{6} - \frac{5 \ln 2}{2} \right) \right] - \frac{\varepsilon}{4} \mathcal{C}_2^{(d)} \right\} + O(\eta^2, \varepsilon^2)$$
(2.33)

follows from Eqs. (2.30) and (2.31) by inserting Eq. (2.32) and the large τ behavior

$$\frac{K_{\alpha+1}(\sqrt{\tau})}{\tau^{3/2} K_\alpha(\sqrt{\tau})} = \tau^{-3/2} + \frac{d-1}{2} \tau^{-2} + \frac{(d-1)(d-3)}{8} \tau^{-5/2}$$
$$+ O(\tau^{-3}).$$
(2.34)

Since $\mathcal{C}_0$ is related to the surface tension $\Delta \sigma$ it should not depend on the shape of K, i.e., on the value of d. Using, e.g., Eqs. (2.31b), (2.14), and (2.15c) corresponding to a planar wall (i.e., $d=1$), one finds

$$\mathcal{C}_0 = -\frac{\pi}{2} + \frac{\pi}{\sqrt{3}}. \tag{2.35}$$

The evaluation of the coefficients $\mathcal{C}_1^{(d)}$ and $\mathcal{C}_2^{(d)}$ in Eq. (2.32) for $d=D$, 3, and 2 is carried out in Appendix A by extending the method explained after Eq. (2.15c) to the next-to-leading terms. For $d=D$, we have to consider $\mathcal{C}_4(\tau)$ only and find

$$\mathcal{C}_1^{(4)} = -\frac{17}{6} + \frac{15\pi}{4} - \frac{3\sqrt{3}\,\pi}{2}, \tag{2.36a}$$

$$\mathcal{C}_2^{(4)} = -66 + \frac{8011\pi}{128} - \frac{191\sqrt{3}\,\pi}{8}; \tag{2.36b}$$

for $d=3$, we find

$$\mathcal{C}_1^{(3)} = -\frac{17}{9} + \frac{5\pi}{2} - \sqrt{3}\,\pi, \tag{2.37a}$$

$$\mathcal{C}_2^{(3)} = -\frac{551}{15} + \frac{1673\pi}{48} - \frac{40\pi}{\sqrt{3}}; \tag{2.37b}$$

and for $d=2$,

$$\mathcal{C}_1^{(2)} = -\frac{17}{18} + \frac{5\pi}{4} - \frac{\sqrt{3}\,\pi}{2}, \tag{2.38a}$$

$$\mathcal{C}_2^{(2)} = -\frac{221}{15} + \frac{1791\pi}{128} - \frac{43\sqrt{3}\,\pi}{8}. \tag{2.38b}$$

We now determine the surface tension $\Delta\sigma$ and the curvature energies $\Delta\kappa_1$, $\Delta\kappa_2$, and $\Delta\kappa_G$ in the expansion (1.7). To this end we need to generalize this expansion to be applicable to $(D-1)$-dimensional surfaces of general shape with values of D different from 3. According to differential geometry for integer $D \geq 3$ the expansion has again the form (1.7a) and the corresponding curvatures are given by

$$K_m = \frac{1}{2} \sum_{i=1}^{D-1} \frac{1}{R_i} = \frac{d-1}{2} \frac{1}{R} \tag{2.39a}$$

and

$$K_G = \sum_{\substack{\text{pairs} \\ i<j}}^{D-1} \frac{1}{R_i R_j} = \frac{(d-1)(d-2)}{2} \frac{1}{R^2}, \tag{2.39b}$$

where R_i are the $D-1$ principal local radii of curvature.

We briefly outline the argument: Following Ref. [26] the curvature contributions should depend on how the surface is embedded in the space $\mathbb{R}^D$, i.e., they should be derivable from the local extrinsic curvature tensor $\mathbf{K}_{ij} = K_{ij}\mathbf{n}$, where $\mathbf{n}$ is the local unit vector normal to the surface (we only consider orientable surfaces). The principal local radii of curvature R_i are the inverse of the $D-1$ eigenvalues of the matrix (K_{ij}). Therefore K_m, K_m^2, and K_G as defined in Eqs. (2.39) are the only independent scalar quantities to first and second order in $1/R_i$ which can be deduced from K_{ij} and which are invariant under permutations of the indices $i=1,\ldots,D-1$.

The last expressions on the rhs of Eq. (2.39) apply to the surface of a generalized cylinder K with integer $d \leq D$. These expressions hold because the surface of K has $d-1$ finite local radii of curvature $R_i = R$ which allow for $(d-1)(d-2)/2$ different pairings. Note that for $D=3$ Eqs. (2.39) reduce to Eqs. (1.7b) and (1.7c). Applying Eqs. (1.7a) and (2.39) to generalized cylinders K in D dimensions one infers from the definition (1.5) of $Y_{d,D}$ and Eq. (2.1) the general form

$$n_p k_B T R Q_{d,D}(\eta) = \Delta\sigma + \Delta\kappa_1 \frac{d-1}{2} \frac{1}{R} + \left[\Delta\kappa_2 \frac{(d-1)^2}{4} + \Delta\kappa_G \frac{(d-1)(d-2)}{2} \right] \frac{1}{R^2} + O(R^{-3}) \tag{2.40}$$

of Q for small η. Explicit results for $\Delta\sigma$, $\Delta\kappa_1$, $\Delta\kappa_2$, and $\Delta\kappa_G$ follow from the results (2.35)–(2.38) for the coefficients $\mathcal{C}_i^{(d)}$ by comparing Eq. (2.40) with Eq. (2.33). Using $\eta = \mathcal{R}_x^2/(2R^2)$, we find for the surface tension to first order in $\varepsilon = 4-D$

$$\Delta\sigma = n_p k_B T \mathcal{R}_x \sqrt{\frac{2}{\pi}} \left\{ 1 - \frac{\varepsilon}{4} \left[1 - \frac{3\ln 2}{2} + \mathcal{C}_0 \right] \right\}$$

$$\approx n_p k_B T \mathcal{R}_x 0.798(1 - 0.0508\varepsilon) + O(\varepsilon^2). \tag{2.41}$$

Here and in the rest of this subsection by taking $\varepsilon = 1$ one obtains the corresponding estimate for the physical dimension $D=3$. By setting $d=2$, 3, and D in Eq. (2.40), in which the generalization of d to noninteger values is obvious, we find for the curvature energies

$$\Delta\kappa_1 = n_p k_B T \frac{\mathcal{R}_x^2}{2} \left\{ 1 - \frac{\varepsilon}{2} \mathcal{C}_1^{(2)} \right\}$$

$$\approx n_p k_B T \mathcal{R}_x^2 0.5(1 - 0.131\varepsilon) + O(\varepsilon^2), \tag{2.42}$$

$$\Delta\kappa_2 = -n_p k_B T \frac{\mathcal{R}_x^3}{3\sqrt{2\pi}} \left\{ 1 - \frac{\varepsilon}{4} \left[\left(\frac{11}{6} - \frac{5\ln 2}{2} \right) - 8\mathcal{C}_2^{(2)} \right] \right\}$$

$$\approx -n_p k_B T \mathcal{R}_x^3 0.133(1 - 0.0713\varepsilon) + O(\varepsilon^2), \tag{2.43}$$

and finally

$$\Delta\kappa_G = -\Delta\kappa_2 - \varepsilon n_p k_B T \frac{\mathcal{R}_x^3}{3\sqrt{2\pi}} \frac{\mathcal{C}_2^{(3)}}{2}$$

$$\approx n_p k_B T \mathcal{R}_x^3 0.133(1 - 0.177\varepsilon) + O(\varepsilon^2). \tag{2.44}$$

Note that $\Delta\kappa_1$ is fixed by considering only one of the cases $d=2$, 3, and D [we chose $d=2$ in Eq. (2.42)]. However, since $\Delta\kappa_1$ must not depend on the value of d, one derives the two conditions

$$\mathcal{C}_1^{(2)} = \frac{\mathcal{C}_1^{(3)}}{2} = \frac{\mathcal{C}_1^{(4)}}{3}, \tag{2.45a}$$

which must be fulfilled if the expansion (1.7) is consistent up to one-loop order in the EV interaction of the polymer

chains. Similarly, $\Delta\kappa_2$ and $\Delta\kappa_G$ are fixed by considering only two of the cases $d=2$, 3, and D [we chose $d=2$ and 3 in Eqs. (2.43) and (2.44)]. Thus one derives the third condition

$$\mathcal{C}_2^{(4)} = 3[\mathcal{C}_2^{(3)} - \mathcal{C}_2^{(2)}]. \qquad (2.45b)$$

By using the values of $\mathcal{C}_1^{(d)}$ and $\mathcal{C}_2^{(d)}$ as derived in the cases (a), (b), (c) above, one finds that all three conditions (2.45) are indeed fulfilled. This confirms to first order in ε the assumption preceding Eq. (2.32) that the scaling function $Y_{d,D}(x)$ is analytic at $x=0$, and that the Helfrich-type expansion (1.7) is applicable to the present polymer-depletion problem for chains with EV interaction. Considering the involved analytical means which were necessary to derive the coefficients $\mathcal{C}_i^{(d)}$ (see Appendix A), we regard this as a very valuable and important check of our calculation and in addition as strong evidence that the above statements for $Y_{d,D}(x)$ are general properties in $D=3$ which hold beyond the present perturbative treatment.

Note that the EV interaction of the polymer chains reduces the absolute values of the surface tension $\Delta\sigma$ and of the curvature energies $\Delta\kappa_1$, $\Delta\kappa_2$, and $\Delta\kappa_G$ as compared to ideal chains. This trend can be anticipated because the EV interaction of the chain monomers effectively *reduces* the depletion effect of the particle surface (compare, e.g., Ref. [19]). However, the corresponding corrections are relatively small so that the overall behavior is changed only quantitatively. Thus exposing one side of a flexible membrane to a solution of polymers which are depleted by the membrane favors a bending of the membrane surface towards the solution [41] and leads to a weakening of its surface rigidity. The sign of the Gaussian curvature energy $\Delta\kappa_G$ will generally favor surfaces with higher genuses (see the Introduction and I). If the resolution of an experimental setup is high enough to observe these effects quantitatively, the corrections due to the presence of the EV interaction of the polymer chains as compared to the behavior for ideal chains should be detectable. Specifically we consider the experiments for vesicles reported by Döbereiner *et al.* [29]. The intrinsic spontaneous curvature energy κ_1 of the bilayer membrane is to be identified with their quantity $-2\kappa\bar{c}_0/R_A$ [compare Eq. (9) in Ref. [29]]. The difference $\Delta\kappa_1$ [see Eq. (2.42)] should be added in the presence of polymers in the solution. The length R_A is of the order of the size of the vesicle. Upon inserting the values $\kappa\approx 10^{-19}$ J and $\bar{c}_0\approx 10$ (compare Fig. 9 in Ref. [29]) one infers $\kappa_1 R_A\approx -2\times 10^{-18}$ J. On the other hand, for $T=300$ K and $n_p\mathcal{R}_x^3$ of order unity, which means that the polymer solution is still in the dilute regime so that the result (2.42) is valid, one has $\Delta\kappa_1\mathcal{R}_x\approx 2\times 10^{-21}$ J. The size ratio $\mathcal{R}_x/R_A$ is of the order of $1/100\ll 1$ for realistic values $R_A\approx 10$ μm and $\mathcal{R}_x\approx 0.1$ μm. We conclude that $\Delta\kappa_1$ can reach a value up to about 10% of κ_1 in a quantitatively controllable way. This can be expected to lead to observable effects near a shape transition of the vesicle.

Ideal chains lead to the behavior that all contributions in curly brackets on the rhs of the expansion (1.7a) of second and higher order in the curvature *vanish* for the case of a generalized cylinder with $d=3$ and $D\geqslant 3$ arbitrary [compare, e.g., Eqs. (3.9) and (3.11) in I]. This encompasses, in

particular, the three-dimensional sphere for which $d=D=3$. For the contribution of second order in the curvature the reason is a combination of the general property $K_G=K_m^2$ for $d=3$ [compare Eq. (2.39)] with the property $\Delta\kappa_G=-\Delta\kappa_2$ valid for any dimension D if the chains are ideal. However, the last property is rather special and is violated for polymers with EV interaction in D slightly below 4 since Eq. (2.44) implies

$$\Delta\kappa_2 + \Delta\kappa_G = -\varepsilon n_p k_B T \frac{\mathcal{R}_x^3}{3\sqrt{2\pi}} \frac{\mathcal{C}_2^{(3)}}{2}$$

$$\approx -\varepsilon n_p k_B T \mathcal{R}_x^3 0.0141 + O(\varepsilon^2). \qquad (2.46)$$

There is no reason to believe that this violation is removed in $D=3$. Rather the crossover to a behavior $Q_{3,3}\sim(\mathcal{R}_x/R)^{1/\nu}$ for $\mathcal{R}_x/R\to\infty$ with the Flory exponent $\nu\approx 0.588$ [see Eqs. (1.8), (2.1), and Sec. II C] implies infinitely many nonvanishing terms in the small curvature expansion (1.7a) in $D=3$. Thus in the physically important case of the three-dimensional sphere the appearance of the EV interaction does lead to a *qualitative* change.

As an illustration, consider a spherical membrane in the dilute polymer solution with *both* sides of the membrane exposed to the polymers. In this case the contributions to $\Delta\kappa_1 K_m$ in the expansion (1.7a) from each side cancel and Eq. (2.46) implies that for chains with EV interaction the free energy cost for immersing the spherical membrane is *smaller* as compared to a flat membrane with the same area. This is different from the behavior for ideal chains for which the solvation free energies for a spherical and a flat membrane with the same area are equal in this case.

C. Long chains: $Y_{d,D}(x)$ for $x\to\infty$

Figure 2 shows in the (d,D) plane the dashed line $d=1/\nu(D)$ [42]. It separates generalized cylinders K which are relevant perturbations for long polymer chains with EV interaction (such as the strip in $D=2$ or the plate in $D=3$) from those which are irrelevant and for which Eq. (1.11) applies. The latter are located in the shaded region above the line and comprise the disk in $D=2$ and the sphere and the cylinder in $D=3$ and are of main interest here. For the sphere and the cylinder in $D=3$ we show within an expansion in $\varepsilon=4-D$ that the first-order result for $Y_{d,D}(x)$ given by Eqs. (2.30) and (2.1) is consistent with the expected power law (1.8) and we determine the corresponding universal amplitude $A_{d,D}$ to first order in ε for $d=D$, 3, and 2. These results in conjunction with the known value for $A_{2,2}$ in $D=2$ are used in order to derive improved estimates for $A_{3,3}$ and $A_{2,3}$ corresponding to a sphere and a cylinder, respectively, in $D=3$.

The line $d=1/\nu(D)$ itself corresponds to marginal perturbations leading to a behavior which in general is different [43] from Eq. (1.8). We shall discuss neither this nor the crossover from marginal to power-law behavior which may arise for points close above the line. Instead, in the case $d=2$ and $D<4$ we shall obtain the ε expansion of $A_{2,D}$ by analytic continuation in d from the corresponding value for $d>2$.
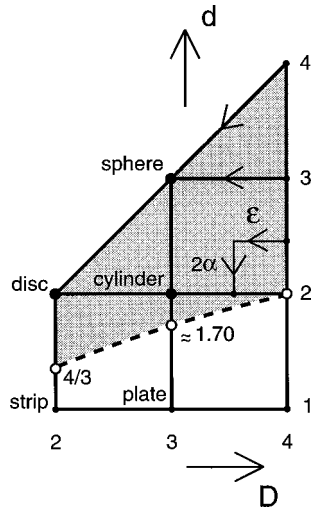
FIG. 2. Diagram of generalized cylinders K which behave—in the renormalization-group sense—as relevant or irrelevant perturbations for nonadsorbing polymers. The parameter $d \leq D$ characterizes the shape of K, and D is the spatial dimension [see Eq. (1.3)]. The point $(d,D) = (2,2)$ corresponds to a disk in $D=2$ and the points (3,3) and (2,3) correspond to a sphere and an infinitely elongated cylinder in $D=3$, respectively. The line with $D=D_{uc}=4$, and arbitrary d represents the upper critical dimension where the polymers behave like ideal chains and from which the perturbative expansion in $\varepsilon = 4 - D$ starts in order to study the effects of the EV interaction. The open circles indicate points (d,D) for which $d - 1/\nu(D) = 0$. These points are connected by the dashed line so that within the shaded region *above* it, the power law (1.8) applies and K represents an irrelevant perturbation. The paths indicated by the arrows are discussed in the main text.

In the following we set d to an arbitrary value with $2 < d \leq D$. By inserting $Q_{d,D}(\eta)$ from Eq. (2.30) in Eq. (2.1) one finds

$$Y_{d,D}(x \to \infty) \to \Omega_d \left[2\alpha\eta - \frac{\varepsilon}{4} C_d(\eta) \right] + O(\varepsilon^2), \quad \eta = x^2/2,$$
(2.47)

where $\alpha = (d-2)/2 > 0$. The first term in square brackets stems from $P_d^{[0]}(\eta)$ in Eq. (2.30b) and $C_d(\eta)$ is given by Eq. (2.31). Both the term Ω_d/d on the rhs of Eq. (2.1) and the sum of the terms following $-C_d(\eta)$ on the rhs of Eq. (2.30c) are subdominant to the leading behavior in Eq. (2.47). According to Appendix A this leads to

$$Y_{d,D}(x \to \infty) \to \Omega_d 2\alpha\eta \left[1 - \frac{\varepsilon}{4}\left(E_d + \frac{\ln\eta}{2} \right) \right] + O(\varepsilon^2)$$

$$= \Omega_d 2\alpha \left[1 - \frac{\varepsilon}{4} E_d \right] \eta \left[1 - \frac{\varepsilon}{4}\frac{\ln\eta}{2} \right] + O(\varepsilon^2).$$
(2.48)

The constant E_d is given by

$$E_d = -\frac{4\pi^2}{\alpha} \mathcal{B}_d - \frac{3}{2} + \ln 2 + \frac{\Psi(d/2)}{2},$$
(2.49)

where for $d=D$ we have to consider E_4 only. The corresponding numbers $\mathcal{B}_d$ are

$$\mathcal{B}_4 = 0, \quad \mathcal{B}_3 \approx 0.010\,47, \quad \mathcal{B}_2 = \frac{1}{8\pi^2}.$$
(2.50)

The result in the second line of Eq. (2.48) for the behavior of $Y_{d,D}(x \to \infty)$ is consistent with the power law (1.8) since

$$\eta^{1/(2\nu)} = 2^{-1/(2\nu)} x^{1/\nu} = \eta\left[1 - \frac{\varepsilon}{4}\frac{\ln\eta}{2} \right] + O(\varepsilon^2) \quad (2.51)$$

[see Eq. (2.24) for $\mathcal{N}=0$]. The universal amplitude $A_{d,D}$ is determined by Eqs. (2.48) and (2.49) to first order in $\varepsilon = 4 - D$ with the results

$$A_{D,D} = 2\pi^2 \left\{ 1 + \frac{\varepsilon}{4}\left[1 - 2\ln\pi - \frac{\ln 2}{2} - \frac{3C_E}{2} \right] \right\}$$

$$\approx 19.739(1 - 0.625\varepsilon) + O(\varepsilon^2),$$
(2.52a)

$$A_{3,D} = 2\pi \left\{ 1 + \frac{\varepsilon}{4}\left[8\pi^2\mathcal{B}_3 + \frac{1}{2} + \frac{\ln 2}{2} + \frac{C_E}{2} \right] \right\}$$

$$\approx 6.283(1 + 0.490\varepsilon) + O(\varepsilon^2),$$
(2.52b)

$$A_{2,D} = \varepsilon 2\pi^3 \mathcal{B}_2 \approx 0.785\varepsilon + O(\varepsilon^2),$$
(2.52c)

where Eq. (2.50) has been used.

From Eq. (2.52c) it is evident that $A_{2,D}$ *vanishes* in the limit $D \nearrow 4$ which reflects the fact that for ideal chains, for which $1/\nu = 2$ and the condition (1.9) is violated, the power law (1.8) does not apply [43]. However, we succeeded in calculating the amplitude $A_{2,D}$ for $D < 4$ to first order in $\varepsilon = 4 - D$ by following a path in the (d,D) plane which circumvents the point (2,4) as indicated by arrows in Fig. 2 and along which the power law (1.8) *does* apply with a positive amplitude $A_{d,D}$. Accordingly, first one has to exponentiate Eq. (2.48) with respect to ε for $\alpha > 0$ fixed in order to obtain the power law (1.8), and then one has to perform the limit $d - 2 = 2\alpha \searrow 0$ for the resulting amplitude $A_{d,D}$ for $D = 4 - \varepsilon$ fixed.

We note that the values for $A_{3,3}$ and $A_{2,3}$ which follow from Eqs. (2.52) by setting $\varepsilon = 1$ are estimates which depend on the path taken. For $\varepsilon = 1$, e.g., Eqs. (2.52a) and (2.52b) lead to the different estimates 7.39 and 9.36, respectively, for the same quantity $A_{3,3}$ [the corresponding paths in the (d,D) plane are indicated by the two upper arrows in Fig. 2]. This discrepancy is caused by the present perturbative calculation of $A_{d,D}$.

This unpleasant feature can be cured. As mentioned in Sec. I B, the power law (1.8) is a special consequence of the small radius expansion (SRE) in Eq. (1.11). Via the polymer magnet analogy, this operator expansion is related to a corresponding SRE in a field theory. This allows one to understand not only the mechanism behind the SRE in terms of perturbative field theoretic methods for D slightly below 4 (as demonstrated in Appendix B) but also to use nonperturbative methods for $D=2$ [44] which incorporate the result $A_{2,2} = 3.81$ (see the end of Appendix B). Improved estimates for the amplitudes $A_{3,3}$ and $A_{2,3}$ can be deduced by combin-
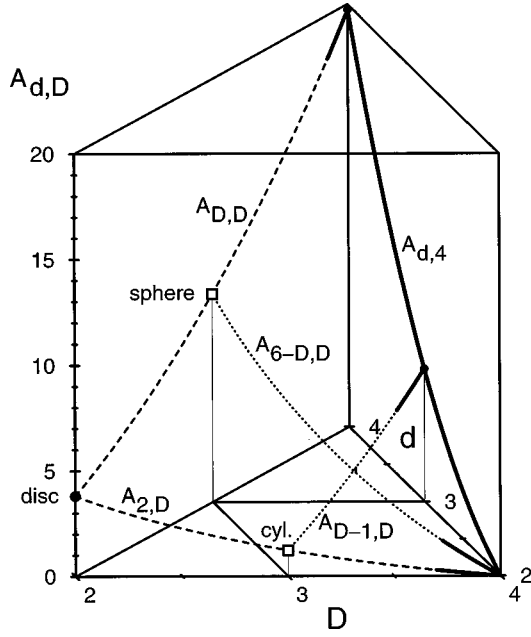
FIG. 3. The universal amplitude $A_{d,D}$ corresponds to a two-dimensional surface over the base plane (d,D) (compare Fig. 2). The full dot corresponding to $A_{2,2}$ and the thick solid lines represent the known parts of this surface. The solid parts of the dashed and of the dotted lines indicate the slopes of these lines at their end points $D=4$ according to Eq. (2.52). The dashed lines themselves including the desired estimates for $A_{3,3}$ and $A_{2,3}$ (open squares) display the corresponding mean values $f_m(\varepsilon)=[f_a(\varepsilon)+f_b(\varepsilon)]/2$ of the two interpolation schemes described in Eq. (2.53). The same holds for the dotted lines and for the two values of $A_{d,D}$ for $(d,D)=(2.5,3.5)$, which have been calculated for a self-consistency check. These two values are connected by the short full line in order to indicate the deviation caused by the fact that the two dotted lines miss each other slightly (for the exact surface $A_{d,D}$, of course, the two dotted lines do intersect at this point). The smallness of the deviation underscores the reliability of the interpolation scheme.

ing the ε expansion of $A_{d,D}$ in Eq. (2.52) with the above value for $A_{2,2}$. To this end we assume that $A_{d,D}$ is a smooth function of d and D. We consider the following interpolation schemes [45] for the functions $f(\varepsilon=4-D)=A_{D,D}$, $A_{2,D}$, $A_{D-1,D}$, and $A_{6-D,D}$, which appear as curves in the $A_{d,D}$ surface shown in Fig. 3.

(a) Pure polynomial,

$$f(\varepsilon)=f_a(\varepsilon)\equiv f(0)+a_1\varepsilon+a_2\varepsilon^2. \qquad (2.53a)$$

(b) (1,1)-Padé form,

$$f(\varepsilon)=f_b(\varepsilon)\equiv f(0)+\frac{b_1\varepsilon}{1+b_2\varepsilon}. \qquad (2.53b)$$

For $A_{D,D}$ and $A_{2,D}$ the coefficients on the rhs of Eqs. (2.53) are fixed by Eqs. (2.52a) and (2.52c), respectively, in conjunction with $f(2)=A_{2,2}$. Note that the corresponding paths in the (d,D) plane are straight lines, i.e., in particular *smooth* paths, so that $A_{d,D}$ behaves smoothly as a function of ε along these paths (see Fig. 3). We obtain estimates for $A_{3,3}$ and $A_{2,3}$ by the corresponding mean values $f_m(\varepsilon)=[f_a(\varepsilon)$

$+f_b(\varepsilon)]/2$ for $\varepsilon=1$ and use the difference between the two values $f_a(1)$ and $f_b(1)$ as an estimate for the error. For the sphere this leads to

$$A_{3,3}=9.82\pm0.3 \qquad (2.54)$$

and for the cylinder to

$$A_{2,3}=1.23\pm0.2. \qquad (2.55)$$

So far the ε expansion of $A_{3,D}$ in Eq. (2.52b) has not been used. Now it can serve as a check for the reliability of the interpolation method leading to Eqs. (2.54) and (2.55). In combination with the known curve $A_{d,4}=2\pi^{d/2}/\Gamma[(d-2)/2]$, Eq. (2.52b) determines the plane tangent to the $A_{d,D}$ surface at $(d,D)=(3,4)$ which leads together with the value for $A_{2,3}$ in Eq. (2.55) to approximations of the form (2.53) for the curve $A_{D-1,D}$. Corresponding approximations for the curve $A_{6-D,D}$ follow from the known tangent plane at $(d,D)=(2,4)$ and the value for $A_{3,3}$ in Eq. (2.54). The resulting mean values $f_m(\varepsilon)$ are shown as dotted lines in Fig. 3. A satisfactory self-consistency check for the accuracy is provided by the observation that at the particular point $(d,D)=(2.5,3.5)$ at which the two exact dotted lines should cross, the approximate ones in Fig. 3 are only slightly off by the small amount of 0.3.

D. The complete scaling function $Y_{3,3}(x)$

The full scaling function $Y_{d,D}(x)$ describes the crossover between its analytic behavior for $x=\mathcal{R}_x/R\to0$ and the power law (1.8) for $x\to\infty$ as discussed in Secs. II B and II C, respectively. Here we consider the complete function $Y_{3,3}(x)$ corresponding to a sphere in $D=3$. The global behavior of $Y_{d,D}(x)$ is conveniently characterized in terms of the function

$$\Theta_{d,D}(x)=\frac{1}{x}\left[Y_{d,D}(x)-\frac{\Omega_d}{d}\right]=\Omega_d\frac{Q_{d,D}(\eta)}{x}, \quad \eta=x^2/2,$$
$$(2.56)$$

where $Q_{d,D}(\eta)$ is defined in Eq. (2.2). According to Eq. (2.40), the value $\Theta_{d,D}(0)$ is related to the surface tension $\Delta\sigma$ in the Helfrich-type expansion (1.7) and the first and second derivatives of $\Theta_{d,D}(x)$ at $x=0$ are related to the corresponding first- and second-order curvature contributions, respectively (compare Sec. II B). In the opposite limit $x\to\infty$ the function $\Theta_{d,D}(x)$ exhibits the power law

$$\Theta_{d,D}(x\to\infty)\to A_{d,D}x^{1/\nu-1} \qquad (2.57)$$

as implied by Eqs. (2.56) and (1.8).

In order to derive an estimate for $\Theta_{3,3}(x)$ we consider the path $d=D$ [compare the derivation of Eq. (2.54)] and introduce a function $F(x,\varepsilon)$ by

$$\Theta_{D,D}(x)=A_{D,D}[F(x,\varepsilon)]^{1/\nu-1}. \qquad (2.58)$$

Both the leading behavior for large x, i.e., $F(x\to\infty,\varepsilon)\to x$, and the small x behavior of F are determined by *integer* powers of x. Due to the corresponding absence of terms $\sim\ln x$ in the ε expansion
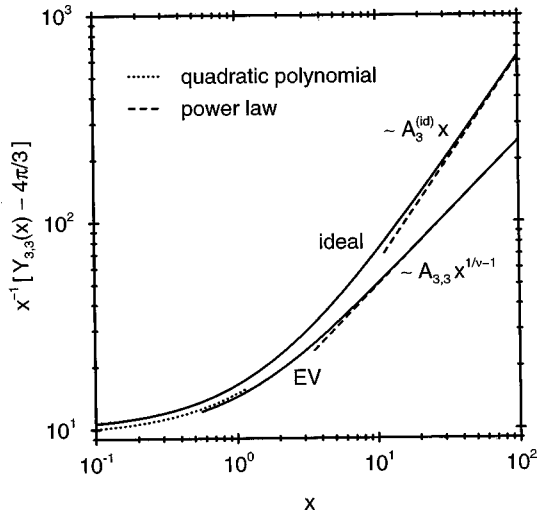
FIG. 4. Scaling function $\Theta_{3,3}(x)=x^{-1}[Y_{3,3}(x)-4\pi/3]$ for the solvation free energy of a sphere in three dimensions [compare Eqs. (1.5) and (2.56) with $\Omega_3=4\pi$]. The lines labeled ''ideal'' correspond to ideal chains and the lines labeled ''EV'' correspond to chains with excluded volume interactions between the monomers. The dashed lines display the power law (2.57). For ideal chains $\Theta_{3,3}(x)=4(2\pi)^{1/2}+2\pi x$ happens to be a linear function of x [compare Eqs. (3.9) and (3.11) in I]. For chains with EV interactions the dashed line represents the power law (2.57) with the accepted exponent $\nu=0.588$ in three dimensions and our best estimate $A_{3,3}\simeq9.82$ for the amplitude. The dotted line displays the polynomial quadratic in x, characterizing $\Theta_{3,3}(x\to0)$ for chains with EV interactions [see Eqs. (2.40) and (2.56)]. The small difference between the lower full line and the dotted line for values of x of order 1 reflects the remaining degree of uncertainty contained in our extrapolation of the ε expansion to three dimensions.

$$F(x,\varepsilon)=F_0(x)+\varepsilon F_1(x)+O(\varepsilon^2), \qquad (2.59)$$

a reasonable first estimate for $F(x,1)$ is to truncate Eq. (2.59) after the second term and to set $\varepsilon=1$. By using Eq. (2.58) this leads to the estimate

$$\Theta_{3,3}(x)\approx A_{3,3}[F_0(x)+F_1(x)]^{1/\nu-1}, \qquad (2.60)$$

with $A_{3,3}=9.82$ from Eq. (2.54) and the exponent value $\nu=0.588$ in three dimensions. The functions $F_0(x)$ and $F_1(x)$ can be inferred from Eqs. (2.30) and (2.31), where the inverse Laplace transforms can be carried out numerically (see Table II in Appendix A), and from Eq. (2.52). In particular one needs the first two terms of the ε expansion

$$P_D^{[0]}(\eta)=P_4^{[0]}(\eta)+\varepsilon\left[-\eta+\mathcal{L}_{\tau\to\eta}\left\{\frac{1}{2\tau^2}\frac{[K_0(\sqrt{\tau})]^2}{[K_1(\sqrt{\tau})]^2}\right\}\right]$$
$$+O(\varepsilon^2) \qquad (2.61)$$

of $P_D^{[0]}(\eta)$ in Eq. (2.30b).

The expression on the rhs of Eq. (2.60) is shown in Fig. 4 as the lower full line labeled ''EV.'' By construction it reproduces for $x\to\infty$ the power law (2.57) with the accepted exponent and our best value in Eq. (2.54) for the amplitude $A_{3,3}$. To judge the degree of accuracy of Eq. (2.60) for general x we compare it with the behavior of Eq. (2.56) for small x as predicted by Eqs. (2.40)–(2.44). Note that for $d=3$

fixed and for small x the dependence of $\Theta_{3,D}(x)$ on $\varepsilon=4-D$ is fully captured by the ε dependence of the surface tension $\Delta\sigma$ and of the curvature energies $\Delta\kappa_1$, $\Delta\kappa_2$, and $\Delta\kappa_G$ as given by Eqs. (2.41)–(2.44). Discarding contributions of order ε^2 in Eqs. (2.41)–(2.44) and setting $\varepsilon=1$ in the first-order terms leads to the dotted line in Fig. 4. The dotted line and the lower full line deviate only slightly from each other and should both provide a rather accurate estimate for the scaling function $Y_{3,3}(x)$.

Figure 4 shows both the behavior for chains with EV interaction and for ideal chains. It is evident that the power law (2.57) not only determines the asymptotic behavior of the scaling function for $x\to\infty$ but it also influences the behavior down to values of x of order unity. This implies that for a quantitative analysis it is indispensable to take the behavior (2.57) into account, in particular the accurate value of the amplitude $A_{3,3}$. Note that $\Theta_{3,3}(x)$ exhibits smaller values for chains with EV interaction than for ideal chains. This is consistent with the exponent $1/\nu-1\approx0.70$ for chains with EV interaction being smaller than the exponent $1/\nu-1=1$ for ideal chains. This difference in behavior is in accordance with the general observation that the EV interaction effectively reduces the depletion effect of the immersed particle (compare the related discussions in Secs. II B and II C).

III. DEPLETION INTERACTION BETWEEN PARTICLES

First, we consider the effective interaction between a thin rod and a planar wall confining the polymer solution. This is another example which demonstrates the importance of the qualitative difference between the behavior for ideal chains and chains with EV interaction which we have discussed in Sec. I B. Then, we consider the effective interaction between two or three small spherical particles in the unbounded solution. When R is small compared with $\mathcal{R}_x$ and the distances between the particles, the small radius expansion (1.11) applies. On the other hand, if both R and some of these distances are small compared to $\mathcal{R}_x$ and the remaining distances, operator expansions slightly more complicated than Eq. (1.11) are expected to hold. In particular, we shall consider a ''small dumbbell'' expansion for two spheres. Finally, we compare our results with those of the PHS model [5].

A. Interaction of a thin rod with a planar wall

In view of the depletion-driven adsorption of colloidal rods onto a hard wall [46], it is of interest to consider a cylinder with radius R and length l immersed parallel to and at a distance $\mathcal{D}$ of closest approach surface-to-surface from a planar wall W in a dilute polymer solution (compare I). We consider the special case $R\ll\mathcal{D},\mathcal{R}_x$ and $\mathcal{D},\mathcal{R}_x\ll l$. Using Eq. (4.19) in I we obtain the corresponding effective free energy of interaction in three dimensions,

$$\Delta F_{\text{depl}}(\mathcal{D})=-n_pk_BTA_{2,3}lR^2(\mathcal{R}_x/R)^{1/\nu}[1-M_M^{(W)}(\mathcal{D}/\mathcal{R}_x)], \qquad (3.1)$$

with the number density n_p of the polymers in the bulk solution and the bulk normalized density profile $M_M^{(W)}(z/\mathcal{R}_x)$ of chain monomers in the half-space (without the cylinder) as a function of the distance z from the wall W. This univer-

TABLE I. Numerical values of the small sphere amplitude $A_{D,D}$ and of the short-distance amplitude σ for chains with EV interaction and for ideal chains.

D	4	3	2	1
$A_{D,D}$	19.739	9.82 ± 0.3	3.810	(marginal)
$A_D^{(id)}$	19.739	6.283	0 (marginal)	
σ	0.101	0.13	0.278	1
$\sigma^{(id)}$	0.101	0.318	∞ (marginal)	

sal density profile can be determined experimentally, e.g., by neutron reflectivity [47] (compare also Fig. 5 in I). Note that Eq. (3.1), in which the universal amplitude $A_{2,3}$ enters [see Eq. (2.55)], is only valid for chains with EV interaction. Equation (3.1) gives rise to an *attractive* interaction between the rod and the wall. The rhs of Eq. (3.1) is fixed by well-defined quantities and is independent of nonuniversal model parameters [48].

For a dilute solution of long rods with $R \ll \mathcal{R}_x \ll l$, Eq. (3.1) determines the enrichment of the rod number density $c(\mathcal{D})$ which occurs at a distance $\mathcal{D}$ from the wall of the order of $\mathcal{R}_x$. Arguing as in the derivation of Eq. (11) in Ref. [46], one finds

$$c(\mathcal{D}) \approx 2(c_b \mathcal{D}/l) \exp[-\Delta F_{depl}(\mathcal{D})/k_B T], \qquad (3.2)$$

where c_b is the number density of the rods in the bulk solution.

B. Depletion interaction between spherical particles

In Eqs. (1.16)–(1.18) the interaction between small spherical particles is expressed in terms of the universal small sphere amplitude $A_{D,D}$ and the monomer density correlation functions C_m of a polymer chain in unbounded infinite space. Numerical values of the former for several spatial dimensions D are summarized in Table I. For the latter we note the relations

$$\int_{\mathbb{R}^D} d^D r_A C_2(\mathbf{r}_A, \mathbf{r}_B) = \mathcal{R}_x^{2/\nu} \qquad (3.3)$$

and

$$\int_{\mathbb{R}^D} d^D r_C C_3(\mathbf{r}_A, \mathbf{r}_B, \mathbf{r}_C) = \mathcal{R}_x^{1/\nu} C_2(\mathbf{r}_A, \mathbf{r}_B), \qquad (3.4)$$

which follow from the defining Eqs. (1.13) and (1.17). Simple limiting behaviors arise if the relative distance $r_{AB} = |\mathbf{r}_A - \mathbf{r}_B|$—albeit being large on the microscopic scale—is much smaller than other mesoscopic lengths. For the pair correlation [15,17,18,49] this limiting behavior takes the form

$$C_2(\mathbf{r}_A, \mathbf{r}_B) \rightarrow \sigma r_{AB}^{-(D-1/\nu)} \mathcal{R}_x^{1/\nu}, \quad r_{AB} \ll \mathcal{R}_x. \qquad (3.5)$$

For the triple correlation, one finds

$$C_3(\mathbf{r}_A, \mathbf{r}_B, \mathbf{r}_C) \rightarrow \sigma r_{AB}^{-(D-1/\nu)} C_2\left(\frac{\mathbf{r}_A + \mathbf{r}_B}{2}, \mathbf{r}_C\right),$$

$$r_{AB} \ll \mathcal{R}_x, |\mathbf{r}_C - (\mathbf{r}_A + \mathbf{r}_B)/2|. \qquad (3.6)$$

Here σ is a universal bulk amplitude. For ideal chains, $\sigma = \sigma^{(id)}$ is only defined for spatial dimensions $D > 2$ for which

$$\sigma^{(id)} = \pi^{-D/2} \Gamma\left(\frac{D}{2} - 1\right). \qquad (3.7)$$

For chains with EV interaction, however, σ remains finite down to $D = 1$. Numerical values of σ for several D are summarized in Table I. In Appendix C we show how these values can be obtained.

For ideal chains the correlation functions C_2 and C_3 can be calculated in closed form. For the pair correlation, one finds for arbitrary D,

$$C_2^{(id)}(\mathbf{r}_A, \mathbf{r}_B) = \pi^{-D/2} \mathcal{R}_x^2 r_{AB}^{2-D} \left[\Gamma\left(\frac{D}{2} - 1, \varrho^2\right) \right.$$
$$\left. - \varrho^2 \Gamma\left(\frac{D}{2} - 2, \varrho^2\right) \right] \qquad (3.8)$$

with Γ the incomplete gamma function [38] and $\varrho^2 = r_{AB}^2/(2\mathcal{R}_x^2) = z_{AB}^2/2$. For $D = 3$, Eq. (3.8) reduces to

$$C_2^{(id)}(\mathbf{r}_A, \mathbf{r}_B) = \pi^{-3/2} (\mathcal{R}_x/z_{AB}) S(z_{AB}^2/2), \qquad (3.9)$$

where

$$S(\varrho^2) = (1 + 2\varrho^2)\sqrt{\pi}\, \text{erfc}\, \varrho - 2\varrho \exp(-\varrho^2) \qquad (3.10)$$

is the Fourier transform of the Debye scattering function [15,17,18]. For the triple correlation one finds in $D = 3$

$$C_3^{(id)}(\mathbf{r}_A, \mathbf{r}_B, \mathbf{r}_C) = \frac{1}{2\pi^{5/2}} \left[\frac{S[(z_{BA} + z_{AC})^2/2]}{z_{BA} z_{AC}} \right.$$
$$+ \frac{S[(z_{AB} + z_{BC})^2/2]}{z_{AB} z_{BC}}$$
$$\left. + \frac{S[(z_{AC} + z_{CB})^2/2]}{z_{AC} z_{CB}} \right]. \qquad (3.11)$$

One can verify that the expressions (3.9) and (3.11) obey the short distance relations (3.5) and (3.6) with $\sigma^{(id)} = \pi^{-1}$ from Eq. (3.7).

The limiting behavior (1.16) ceases to apply if the mutual distance between the small spheres becomes comparable with the order of their radii. As an illustration we consider two spheres A and B with equal radii $R_A = R_B = R$. While for $R \ll r_{AB}, \mathcal{R}_x$ the reduced free energy of interaction $n_p f_{A,B}^{(2)}$ is given by Eq. (1.16a) and, in particular, for $R \ll r_{AB} \ll \mathcal{R}_x$ by

$$f_{A,B}^{(2)} \rightarrow -(A_{D,D})^2 \sigma R^{2(D-1/\nu)} \mathcal{R}_x^{1/\nu} r_{AB}^{-(D-1/\nu)} \qquad (3.12)$$

due to Eq. (3.5), one finds for $R, r_{AB} \ll \mathcal{R}_x$ with arbitrary r_{AB}/R that

$$f_{A,B}^{(2)} \rightarrow -(2 - \mathcal{M}) A_{D,D} R^{D-1/\nu} \mathcal{R}_x^{1/\nu}. \qquad (3.13)$$

Here

$$\mathcal{M} = \mathcal{M}(\mathcal{D}/R) \qquad (3.14)$$

is independent of $\mathcal{R}_x$ and is a universal function of $\mathcal{D}/R$ with

$$\mathcal{D} = r_{AB} - 2R \qquad (3.15)$$

the distance of closest approach surface-to-surface between the two spheres A and B. Equation (3.13) holds because on the large length scale set by $\mathcal{R}_x$ the "dumbbell" composed of the two spheres with small R and $\mathcal{D}$ can be considered in leading order [50] as a pointlike perturbation as in Eq. (1.11) in conjunction with the lower part of Eq. (1.12), but with the amplitude $A_{D,D}$ replaced by an amplitude function $\mathcal{M}A_{D,D}$ which depends on $\mathcal{D}/R$. Consistency of Eqs. (3.13) and (3.12) requires that

$$2 - \mathcal{M} \to A_{D,D}\sigma(\mathcal{D}/R)^{-(D-1/\nu)}, \quad \mathcal{D}/R \to \infty. \quad (3.16)$$

In the opposite limit $\mathcal{D}/R \to 0$ of two *touching* spheres [19](b) the function $\mathcal{M}(\mathcal{D}/R)$ approaches a constant larger than 1 because the dumbbell is a stronger perturbation than a single sphere. This small dumbbell operator expansion can be used for a calculation not only of the solvation free energy of the dumbbell but also of other observables such as the monomer density profile at distances from the dumbbell which are much larger than R and $\mathcal{D}$.

Similar to the small radius expansion (1.11) the small dumbbell expansion has—via the polymer magnet analogy—its counterpart in the $\mathcal{N}$-component field theory. An easy way to obtain the explicit expression for $\mathcal{M}A_{D,D}$ is to calculate the energy density profile $\langle -\boldsymbol{\Phi}^2(\mathbf{r})\rangle_{\text{db, crit}}$ *at the critical point* of the field theory in the presence of the two spheres with radius R and Dirichlet boundary conditions which represent the dumbbell (db) centered at the origin, and to compare the result with the corresponding result as derived from the small dumbbell expansion in the form

$$\mathcal{M}A_{D,D} = \lim_{r \to \infty} \frac{\langle -\boldsymbol{\Phi}^2(\mathbf{r})\rangle_{\text{db, crit}} - \langle -\boldsymbol{\Phi}^2\rangle_{b,\text{crit}}}{R^{D-1/\nu}\langle \Psi(0)\boldsymbol{\Phi}^2(\mathbf{r})\rangle_{b,\text{crit}}}. \quad (3.17)$$

Here Ψ is the normalized energy density introduced in Eq. (C7) and the rhs of Eq. (3.17) is taken in the limit $\mathcal{N} \searrow 0$. The evaluation of the numerator is simplified by means of a conformal transformation relating it to the corresponding quantity between two *concentric* spheres [34](b).

For ideal chains—corresponding to a Gaussian field theory—the latter quantity is known and leads to

$$\mathcal{M} = 2(\theta^{-1/2} - \theta^{1/2})^{D-2}\sum_{l=0}^{\infty}\binom{D-3+l}{l}$$

$$\times[\theta^{-[l+(D-2)/2]} + 1]^{-1}, \qquad (3.18a)$$

where θ is related to the dumbbell parameter $\mathcal{D}/R$ via

$$\frac{1}{2}(\theta + \theta^{-1}) = 1 + 2\frac{\mathcal{D}}{R} + \frac{1}{2}\left(\frac{\mathcal{D}}{R}\right)^2. \qquad (3.18b)$$

Equation (3.18) provides an explicit expression for $f_{A,B}^{(2)}$ in Eq. (3.13). In particular, one can check Eq. (3.16) by using the relations $A_{D,D}^{(\text{id})}\sigma^{(\text{id})} = 2$ and $\nu^{-1} = 2$ valid for ideal chains. In $D=3$ one finds the leading behavior [51]

$$\lim_{\mathcal{R}_x \to \infty} \frac{f_{A,B}^{(2)}}{2f_A^{(1)}} \to -(1 - \ln 2) + \frac{\mathcal{D}}{R}\frac{1}{6}\left(\ln 2 - \frac{1}{4}\right), \quad \mathcal{D}/R \to 0, \quad (3.19)$$

which determines not only the solvation free energy of, but also the depletion force between, two small touching spheres in a dilute solution of ideal chains in $D=3$. Numerical evaluation of Eq. (3.18) for *arbitrary* $\mathcal{D}/R$ in $D=3$ shows that the crossover of $f_{A,B}^{(2)}/(2f_A^{(1)})$ from the behavior given on the rhs of Eq. (3.19), valid for $\mathcal{D} \ll R \ll \mathcal{R}_x$, to the behavior $-R/\mathcal{D}$, valid for $R \ll \mathcal{D} \ll \mathcal{R}_x$, is monotonic and without inflection point. Since this holds also for the crossover from $R \ll \mathcal{D} \ll \mathcal{R}_x$ to $R \ll \mathcal{R}_x \ll \mathcal{D}$ as implied by Eqs. (3.9) and (1.16a), one finds that upon increasing the distance $\mathcal{D}$ the reduced free energy of interaction $n_p f_{A,B}^{(2)}$ between two small spheres is monotonically increasing and the attractive force $(\partial/\partial\mathcal{D})n_p f_{A,B}^{(2)}$ is monotonically decreasing in the whole range of $\mathcal{D}$.

This is different from the behavior of a particle with small radius interacting with a *planar wall* (compare Sec. III A and I). In this case the attractive force $(\partial/\partial\mathcal{D})\Delta F_{\text{depl}}$ is not monotonically decreasing with increasing $\mathcal{D}$ but exhibits a *maximum* at a distance $\mathcal{D}_{\max}$ of the order $\mathcal{R}_x$ since the monomer density profile $M_M^{(W)}$ in Eq. (3.1) has a point of inflection. This qualitatively different feature applies not only to a thin cylinder but also to a small spherical particle near a wall [52]. Another remarkable difference between the two cases is the behavior of the force in the limit $R, \mathcal{D} \ll \mathcal{R}_x$. While in the case of two spheres $(\partial/\partial\mathcal{D})n_p f_{A,B}^{(2)}$ increases as $\mathcal{R}_x^{1/\nu}$ for $\mathcal{R}_x \to \infty$, the force $(\partial/\partial\mathcal{D})\Delta F_{\text{depl}}$ between the particle and the wall exhibits a *finite* limit for $\mathcal{R}_x \to \infty$. This is plausible since the particle eventually moves into a region which is already depleted due to the presence of the wall.

It is interesting that for two touching spheres in a solution of ideal chains in $D=3$ the form of the normalized interaction free energy

$$f_{A,B}^{(2)}/(2R)^3 = -\frac{a}{2}(\mathcal{R}_x/R)^2, \quad R \ll \mathcal{R}_x, \quad (3.20a)$$

for *small* radius as implied by Eqs. (3.19), (1.5), (1.8), and $A_3^{(\text{id})} = 2\pi$ is very similar to its counterpart

$$f_{A,B}^{(2)}/(2R)^3 = -\frac{b}{2}(\mathcal{R}_x/R)^2, \quad R \gg \mathcal{R}_x, \quad (3.20b)$$

for *large* radius following from the Derjaguin approximation [53], which is supposed to be exact in this limit. Both forms display the same power in the length ratio $\mathcal{R}_x/R$ and their amplitudes $a = \pi(1 - \ln 2) = 0.964$ and $b = (\pi/2)\ln 2 = 1.09$ are nearly the same. Although we do not have an explicit expression for the normalized interaction free energy for $\mathcal{R}_x/R$ of order unity, we expect that either of the two limiting forms (3.20) provides a reasonable approximation even in the intermediate regime. This is confirmed by the computer simulation results of Ref. [12] in which the chain is modeled as an N-step random walk on a simple cubic lattice with $N=10$ or 100 and the diameter $2R$ of each of the two touching spheres equals 10.5 lattice constants. This corresponds to the values 0.06 or 0.60 of $\frac{1}{2}(\mathcal{R}_x/R)^2$

$= \frac{1}{6} N/(\frac{1}{2} 10.5)^2$ and each of our two forms leads to estimates which are fairly close [54] to the simulation results 0.04 or 0.50 displayed in Fig. 3 of Ref. [12] for the quantity $-\bar{\Omega}^{2b}*/\sigma_{\mathrm{col}}^3$ there, which is to be identified with $-f_{A,B}^{(2)}/(2R)^3$ here.

In order to be able to appreciate the results for the depletion interaction of particles with small radii R as obtained in this subsection, it is instructive to compare them with those of the PHS model [5] extrapolated to the case of small R [55]. A force displaying a maximum at a distance $\mathcal{D}_{\max}$ of order $\mathcal{R}_x$ for the effective interaction between a particle and a planar wall and a monotonical decrease of the force with increasing $\mathcal{D}$ for two particles of equal size are also found within the PHS model when extrapolated to $R \ll \mathcal{R}_x$. However, the PHS model does not produce the decrease of the absolute values of the free energy of interaction and of the force with decreasing R but in the limit $R \to 0$ rather leads to finite quantities which are independent of R. For example, in the case of a thin cylinder or a small sphere near a wall the maximum force in the PHS model is not proportional to $R^{d-1/\nu} \mathcal{R}_x^{1/\nu-1}$ as for a flexible chain but rather to $\mathcal{R}_x^{d-1}$. In the particle-wall case the PHS model also fails to predict that the force becomes independent of $\mathcal{R}_x$ for $R, \mathcal{D} \ll \mathcal{R}_x$.

Even for the much studied case of a *large* sphere radius, i.e., $R \gg \mathcal{R}_x$, for which the PHS approximation is expected to work best, the deviation of the PHS approximation from the Derjaguin result is considerable. The PHS approximation implies $b = 1$ in Eq. (3.20b) [56], i.e., it leads to a free energy $f_{A,B}^{(2)}$ for two large touching spheres of equal size whose absolute value is too small by about 10 %. The same ratio $(\pi/2)\ln 2$ between the Derjaguin result and the PHS approximation appears in the case of a single large sphere touching a planar wall (compare footnote [28] in Ref. [57]).

IV. SUMMARY AND CONCLUDING REMARKS

We have studied the interaction of mesoscopic particles (spheres, cylinders, and planar walls) with a dilute solution of long, flexible, free, and nonadsorbing polymer chains which are depleted by the particles in good or theta solvents. The properties for a single particle as well as the effective interaction between two or more particles have been considered.

One topic of main concern has been to investigate in a systematic and quantitative way how the excluded volume (EV) interaction between the chain monomers modifies the ideal chain behavior. Our results are in line with the plausible conjecture that *weaker* depletion effects arise from chains with EV interaction than from ideal chains with the same Flory radius. Another main topic has been the description of situations in which the particle radius R is small compared with the Flory radius $\mathcal{R}_x$ so that the chain will coil around the particle (compare Fig. 1) and in which the classic PHS treatment ignoring chain flexibility [5] is clearly of no use. For example, consider the limit $R/\mathcal{R}_x \to 0$ in which the spherical or cylindrical particle degenerates to a point or a thin needle, respectively, on the scale of $\mathcal{R}_x$: for flexible polymers both the solvation free energy of the particle and its polymer-mediated free energy of interaction with other particles vanishes in this limit, whereas these two quantities

remain finite for the rigid polymers of the PHS model.

Our analysis is based on the polymer magnet analogy which maps the polymer problem with interactions within a single polymer chain and between a polymer chain and a particle onto a Ginzburg-Landau $(\Phi^2)^2$ field theory in the outer space of the particle with the order parameter field Φ vanishing on the particle surface (see Ref. [19], I, and Sec. II A). This allows us to resort to basic field-theoretical tools such as the renormalization-group and short-distance expansions which turn out to be extremely useful for the understanding of the polymer conformations in the presence of the particle(s).

In the following we summarize our main results starting with the case of a single particle. The evaluation in I of the solvation free energy for immersing the particle in a theta solvent (i.e., ideal chains) has been generalized to the generic case of a good solvent (i.e., chains with EV interaction) by calculating the universal scaling function $Y_{d,D}(\mathcal{R}_x/R)$ [see Eq. (1.5)]. For estimates based on a systematic perturbative approach it is useful to introduce the particle shape of a "generalized cylinder" [see Eq. (1.3)] which is characterized by the space dimension D and an internal dimension d encompassing cylinder, sphere, and wall as special cases. The general results for $Y_{d,D}(x)$ to first order in $\varepsilon = 4 - D$ are given by Eqs. (2.1) and (2.30).

(i) Our investigations in Sec. II B of generalized cylinders with small curvature, i.e., $R \gg \mathcal{R}_x$, provide strong evidence for the validity of the local and analytic Helfrich-type expansion conjectured in Eq. (1.7). With the help of Eq. (2.39) this expansion can be generalized to arbitrary spatial dimensions D so that we were able to obtain explicit expressions for the universal coefficients $\Delta\sigma$, $\Delta\kappa_1$, $\Delta\kappa_2$, and $\Delta\kappa_G$ appearing in the Helfrich Hamiltonian to first order in $\varepsilon = 4 - D$. While the results for the spontaneous curvature energy $\Delta\kappa_1$ in Eq. (2.42) and the mean and Gaussian bending rigidities $\Delta\kappa_2$ and $\Delta\kappa_G$ in Eqs. (2.43) and (2.44) are new, the result in Eq. (2.41) for the surface tension $\Delta\sigma$ has implicitly been noted before [see Eq. (4.7) in Ref. [58]]. All coefficients have absolute values smaller than those of their ideal chain counterparts. The latter are given by the above expressions for $\varepsilon = 0$. The decrease of the depletion effects due to the EV interaction can be traced back to a corresponding behavior of the profile M_E of the end density [see Eqs. (2.1) and (2.2)]. The simplest case is the surface tension $\Delta\sigma$ which follows from the profile M_E near a planar wall and for which the decrease is consistent with a corresponding decrease [19](a) of the surface exponent a_E in the behavior $M_E \sim (z/\mathcal{R}_x)^{a_E}$ for distances z from the wall much smaller than $\mathcal{R}_x$.

(ii) For small particle radius, i.e., $R \ll \mathcal{R}_x$, our results for $Y_{d,D}(x)$ to first order in ε confirm the validity of the power law (1.8) within the region (1.9) and allow us to determine the ε expansions of the universal amplitude $A_{d,D}$ [see Eq. (2.52)]. The region (1.9) is shown shaded in Fig. 2 and includes the interior point $(d,D) = (2,3)$ which represents a cylinder in three dimensions. This is different from the case of ideal chains in which Eqs. (1.8) and (1.9) are not valid below and on the line $d = 2$. Reliable estimates for the amplitudes $A_{3,3}$ and $A_{2,3}$ corresponding to a sphere and a cylinder, respectively, for chains with EV interaction in three dimensions have been obtained from the plausible assumption that the amplitude $A_{d,D}$ as a function of d and D forms a

regular surface over the base plane (d, D) (see Fig. 3). The combination of the value of $A_{2,2}$ corresponding to a disk in two dimensions (see Table I) with the ε expansions of $A_{d,D}$ in Eq. (2.52) leads to the estimates in Eqs. (2.54) and (2.55) for $A_{3,3}$ and $A_{2,3}$.

(iii) An estimate of the full scaling function $Y_{3,3}(x)$ for the solvation free energy of a sphere in three dimensions is shown in Fig. 4 in terms of the function $\Theta_{3,3}(x)$ [see Eq. (2.56)]. This shows the crossover from the small curvature regime $x \ll 1$ with the coefficients $\Theta(0)$, $\Theta'(0)$, and $\Theta''(0)$ of its Taylor expansion about the regular point $x = 0$ being simply related to the surface tension $\Delta\sigma$, the energy $\Delta\kappa_1$ of spontaneous curvature, and the bending rigidities $\Delta\kappa_2$ and $\Delta\kappa_G$, respectively [see Eqs. (2.40) and (2.56)], to the small radius regime $x \gg 1$ with the power law $\Theta_{3,3}(x \to \infty) \to A_{3,3}x^{1/\nu-1}$. As expected, the curve for chains with EV interaction is *below* the corresponding curve for ideal chains which implies a smaller solvation energy. For chains with EV interaction the exponent $1/\nu - 1$ is not a positive integer and the expansion of $\Theta_{3,3}(x)$ or $Y_{3,3}(x)$ about $x = 0$ cannot be a polynomial with a finite number of terms. This is in contrast with the solvation free energy of a sphere in a solution of ideal chains in which case $\Theta(x)$ is a linear function of x (see Ref. [11] or I).

We continue by summarizing our results for the interaction between particles with a small radius. Since the values in Eqs. (2.54) and (2.55) of the amplitudes $A_{3,3}$ and $A_{2,3}$ completely determine the Boltzmann weight in Eq. (1.11) of a small sphere and a thin cylinder, the interactions of these particles with other distant particles or walls are completely determined, too [34,36,37,52,59].

(iv) We have studied the interaction between a wall and a long thin cylindrical particle a distance $\mathcal{D}$ apart with radius R and length l for the case $R \ll \mathcal{R}_x, \mathcal{D} \ll l$. The dependence on $\mathcal{D}$ of the polymer-mediated free energy of interaction is proportional to that of the monomer density $M_M^{(W)}$ of a dilute solution of chains in the half-space *without* the particle [see Eq. (3.1)]. The same applies for a small sphere near a wall (compare I). Since $M_M^{(W)}$ has a point of inflection at $\mathcal{D} \sim \mathcal{R}_x$, the attractive mean force between a wall and a thin cylinder or between a wall and a small sphere somewhat surprisingly passes through a maximum as $\mathcal{D}$ increases. The increase $\sim \mathcal{D}^{1/\nu-1}$ of the force per unit length l^{D-d} and unit bulk pressure $n_p k_B T$ with the distance $\mathcal{D}$ in the region $R \ll \mathcal{D} \ll \mathcal{R}_x$ is a consequence of its length dimension $d - 1$, its independence of $\mathcal{R}_x$, and of the fact that the particle radius R enters the force only in the form of the power law $R^{d-1/\nu}$ according to Eq. (1.11). Our study of the situation of long chains is complementary to that of short chains, i.e., $\mathcal{R}_x \ll R$, considered in Ref. [46]. In the latter case the attractive mean force of depletion is monotonically decreasing as $\mathcal{D}$ increases.

(v) The interaction between two small spherical particles A, B of equal size and with a distance $r_{AB} = \mathcal{D} + 2R$ between their centers has been studied in Sec. III B both for $R \ll \mathcal{D}, \mathcal{R}_x$ and for $R, \mathcal{D} \ll \mathcal{R}_x$. In the former case we use Eq. (1.16a) expressing the interaction in terms of $A_{D,D}$, R, and the universal monomer density correlation function C_2 of a single chain in unbounded space. In the latter case the "dumbbell" composed of the two spheres is small on the

scale of $\mathcal{R}_x$ and can in leading order be considered as a pointlike object. This gives rise to an expansion similar to Eq. (1.11) in conjunction with the lower part of Eq. (1.12) in which, however, the amplitude $A_{D,D}$ is replaced by an amplitude *function* $\mathcal{M}A_{D,D}$ depending on R and $\mathcal{D}$. This is another type of a short-distance-like operator expansion which can be used not only for the effective free energy of interaction but also for other polymer properties—such as the monomer density profile—induced by the two spheres. Both cases overlap in the region $R \ll \mathcal{D} \ll \mathcal{R}_x$ in which the interaction free energy $f_{A,B}^{(2)}$ per unit bulk pressure $n_p k_B T$ is given by Eq. (3.12). Numerical values of $A_{D,D}$ and the universal bulk amplitude σ in Eq. (3.12) are summarized in Table I for various space dimensions and both for ideal chains and chains with EV interaction. The value for σ in $D = 2$ derived in Appendix C is a new result for a self-avoiding chain in the unbounded plane. For $D = 3$ and ideal chains we explicitly calculate the two functions C_2 and $\mathcal{M}A_{D,D}$ [see Eqs. (3.8) and (3.18)] and thus present a complete and explicit expression for the free energy of interaction between two small spherical particles to leading order in the small quantity $R/\mathcal{R}_x$. In contrast to the polymer-mediated force between a small sphere and a wall, for two spheres of equal size the force is monotonically decreasing in the whole range of $\mathcal{D}$. For the case of two touching spheres and arbitrary values of $R/\mathcal{R}_x$ we consider an approximative form of $f_{A,B}^{(2)}$ [compare Eq. (3.20)] and compare it with the results [12] of simulations.

(vi) As an illustration for the nonpairwise character of the depletion interaction between particles, we have evaluated an explicit analytic expression for the three-particle interaction $f_{A,B,C}^{(3)}$ in the case of small spherical particles and ideal chains in three dimensions. The expression follows by inserting the triple correlation function in Eq. (3.11) of the monomer density in the unbounded solution in Eq. (1.16b) and using that in this case $D - 1/\nu = 1$ and $A_{D,D} = A_3^{(id)} = 2\pi$. The result is valid in the region $R \ll r_{ij}, \mathcal{R}_x$ with r_{ij} denoting the relative distances r_{AB}, r_{AC}, or r_{BC} between the spheres and is complementary to the three-body results presented in Ref. [12] with R of the order of $\mathcal{R}_x$. In order to convey an idea of the relative importance of one-, two-, and three-particle contributions, we summarize the results

$$(f^{(1)}, f_{A,B}^{(2)}, f_{A,B,C}^{(3)}) = 2\pi R \mathcal{R}_x^2 \left(1, -2\frac{R}{r_{AB}}, \right.$$
$$\left. 2R^2 \frac{r_{AB} + r_{BC} + r_{CA}}{r_{AB} r_{BC} r_{CA}} \right) \qquad (4.1)$$

for the special case $R \ll r_{ij} \ll \mathcal{R}_x$. For three small spheres configured on an equilateral triangle with edge length r, the interaction $f_{A,B,C}^{(3)}$ is related to $f_{A,B}^{(2)}$ for two spheres at a distance $2r$ via

$$(f_{A,B,C}^{(3)})_{r_{ij}=r} / (-f_{A,B}^{(2)})_{r_{AB}=2r} = 6R/r. \qquad (4.2)$$

This relation holds for an arbitrary ratio $r/\mathcal{R}_x$ provided $R \ll r, \mathcal{R}_x$.

Another interesting type of three-body depletion interaction arises for two spherical particles near a planar wall. If their radii are small, this situation can again be systemati-

cally investigated by means of Eq. (1.11) and the lower part of Eq. (1.12). In the same spirit the investigations of three-body interactions could be supplemented to cover cases in which the distance between two of the spheres (or between one of the spheres and the wall) becomes of the order of R or smaller by means of the "small dumbbell" expansion (or an expansion which applies to a sphere close to a planar wall [52]).

Finally, we summarize some of the field-theoretic developments on which our treatment of the particle-chain interaction is based.

(vii) After a brief outline of the polymer magnet analogy in Sec. II A we relate for a generalized cylinder K immersed in a dilute polymer solution the density profile M_E of chain ends to the local susceptibility in the corresponding magnetic system [see Eq. (2.27)]. For nonadsorbing chains the corresponding order parameter field $\mathbf{\Phi}$ vanishes at the surface of the particle. With the Gaussian order parameter correlation function outside K as the unperturbed propagator we use renormalized perturbation theory with respect to a $(\mathbf{\Phi}^2)^2$ interaction in order to obtain a systematic expansion in the EV interaction of the polymer quantities below the upper critical dimension $D_{uc}=4$. The behavior of our one-loop expressions [see the function $\mathcal{C}_d(\tau)$ in Eq. (2.31)] in the limits corresponding to large R and small R is discussed in Appendix A.

(viii) We verify to first order in the EV interaction that the *same* small radius amplitude appears for *different* properties of a generalized cylinder with a small radius R. In Appendix B we write Eq. (1.11) in terms of fluctuating densities (operators) in the equivalent field theory. The universal small radius amplitude $A_{d,D}$ for polymers is obtained from a corresponding critical amplitude $\hat{A}_{d,D}$ in the field theory by multiplying with a universal noncritical bulk amplitude. In the two-point correlation function with distances of the two points from the generalized cylinder much larger than R there appears the same amplitude $\hat{A}_{d,D}$ at the critical point of the field theory—where the correlation length ξ_+ is infinitely large—as in the behavior of the field-theoretic excess susceptibility of the generalized cylinder for $\xi_+/R\gg1$. The latter is related to the power-law behavior (1.8) of the function $Y_{d,D}(x)$ for $x=\mathcal{R}_x/R\gg1$. These considerations are important to understand that the mechanism behind the small radius expansion is basically of the same type as that behind the well-known short distance expansions in field theories without boundaries [37,59]. Moreover, in the case of a sphere our result for $\hat{A}_{D,D}$ to first order in ε confirms that this amplitude can be reduced to bulk and half-space amplitudes as predicted from a conformal mapping [60] (see the penultimate paragraph in Appendix B).

(ix) By studying the energy density profile in a Gaussian field theory with boundaries, we explicitly verify that not only a single sphere but also a "dumbbell" composed of two spheres of equal size can be considered as a pointlike perturbation on sufficiently large length scales. At bulk criticality the profile for the dumbbell can be obtained by means of a conformal transformation from the known profile between two concentric spheres. For ideal polymer chains we thus find the explicit form [see Eq. (3.18)] of the amplitude function $\mathcal{M}A_{D,D}$ addressed in paragraph (v) of this Summary.

APPENDIX A: THE FUNCTION $\mathcal{C}_d(\tau)$

The results of Sec. II are based on the behavior of the function $Q_{d,D}(\eta)$ in Eq. (2.30), in particular on the behavior of $C_d(\eta)$ in Eq. (2.31). The difficult part of the corresponding calculation consists in performing the sum over n and the double integral over q and ψ in order to calculate $\mathcal{C}_d(\tau)$ according to Eqs. (2.15b) and (2.31b). Here we derive the asymptotic expansions of $\mathcal{C}_d(\tau)$ for large and small τ, respectively, and give numerical values of $\mathcal{C}_d(\tau)$ for the crossover region $0\lesssim\tau\lesssim3$.

1. $\mathcal{C}_d(\tau)$ for $\tau\to\infty$

We calculate the coefficients $\mathcal{C}_1^{(d)}$ and $\mathcal{C}_2^{(d)}$ in Eq. (2.32) for $d=D$, 3, and 2 by expanding the rhs of Eq. (2.31b) for large τ. To this end we need the behavior of the integrand in Eq. (2.31b) for $R\mu\sqrt{t}=\sqrt{\tau}$ large and $(y_\perp-R)\mu\sqrt{t}=(\psi-1)\sqrt{\tau}\equiv s$ arbitrary. This is consistent with the expectation that for the small curvature expansion the important regime in terms of polymer variables is $R/\mathcal{R}_x$ large and $(y_\perp-R)/\mathcal{R}_x$ arbitrary.

(a) $d=D$. Since $\mathcal{C}_1^{(D)}$ and $\mathcal{C}_2^{(D)}$ belong to the one-loop contribution of $Q_{D,D}(\eta)$, we need to consider only $\mathcal{C}_1^{(4)}$ and $\mathcal{C}_2^{(4)}$ [compare the remarks below Eqs. (2.20) and (2.31b)]. The central part of the calculation consists in expanding $g_s(\psi,\tau,\varepsilon=0)$ in the integrand on the rhs of Eq. (2.31b) for τ large and s arbitrary. Since $W_n^{(1)}(0)=(n+1)^2/(2\pi^2)$ for $\alpha=1$ in Eq. (2.15b), the quantity $g_s(\psi,\tau,0)$ is, apart from a factor $-\psi^2/(2\pi^2)$, given by

$$\sum_{n=0}^\infty n^2 \frac{I_n(\sqrt{\tau})}{K_n(\sqrt{\tau})}[K_n(s+\sqrt{\tau})]^2. \tag{A1}$$

A first hint on how to evaluate the sum (A1) for large τ can be gained from recognizing that its leading behavior corresponding to a vanishing curvature must describe the half-space bounded by a planar wall. This is discussed after Eq. (2.15c) and shows that the ratio n/R has the meaning of the length of a wave vector parallel to the wall and that all values of n are important for which $(n/R)/(\mu\sqrt{t})=n/\sqrt{\tau}\equiv\omega$ or $(n/R)(y_\perp-R)=ns/\sqrt{\tau}$ are of order unity. Thus for the general expansion for large τ a large number of terms will contribute and the sum can be replaced by an integral plus corrections according to the Euler-MacLaurin formula [61]:

$$\sum_{n=0}^\infty F(n)=\int_0^\infty dn F(n)+\frac{1}{2}F(0)-\frac{B_2}{2!}F'(0)$$

$$-\frac{B_4}{4!}F'''(0)+\cdots. \tag{A2}$$

Here B_k are Bernoulli numbers and the function $F(n)$ can be read off from the expression (A1). For case (a) the analysis

of this expression shows that all contributions on the rhs of Eq. (A2) apart from the integral lead to orders of $\tau^{-1/2}$ higher than needed for the first three terms on the rhs of the expansion (2.32) of $\mathcal{C}_4(\tau)$ [but compare case (b) below]. Upon introducing ω instead of n as the integration variable, the expression (A1) turns into

$$\tau^{3/2}\int_0^\infty d\omega\,\omega^2\frac{I_a(a/\omega)}{K_a(a/\omega)}\left[K_a\left(a\frac{s+\sqrt{\tau}}{\omega\sqrt{\tau}}\right)\right]^2 \quad (A3)$$

with $a=\omega\sqrt{\tau}$. For large τ the integral (A3) can be simplified by employing the *uniform* asymptotic expansion for large orders a of the modified Bessel functions I_a and K_a which is provided, e.g., in Eqs. (9.7.7) and (9.7.8) of Ref. [38(a)]. In addition to the leading term [compare the discussion after Eq. (2.15c)], now also the correction terms containing the functions u_0, u_1, and u_2 given in section 9.3.9 of the above reference have to be included. By inserting this simplified integral into g_s in Eq. (2.31b), one finds that the first three coefficients on the rhs of the expansion (2.32) of $\mathcal{C}_4(\tau)$ are determined by a number of double integrals over s and ω which can all be calculated in closed form. This reproduces the expression (2.35) for $\mathcal{C}_0$—and thus checks the assumption leading to it—and yields the expressions for $\mathcal{C}_1^{(4)}$ and $\mathcal{C}_2^{(4)}$ in Eq. (2.36).

(b) $d=3$. Due to the additional integration over q in Eq. (2.15b), the expression corresponding to (A1) now reads $\Sigma_{n=0}^\infty F(n+1/2)$ where, using $W_n^{(1/2)}(0)=(n+1/2)/(2\pi)$ and substituting $\kappa=q\tau^{-1/2}$ in Eq. (2.15b),

$$F(n)=\sqrt{\tau}n\int_0^\infty d\kappa\,\frac{I_n(\sqrt{\tau}\sqrt{\kappa^2+1})}{K_n(\sqrt{\tau}\sqrt{\kappa^2+1})}\{K_n[(s+\sqrt{\tau})\sqrt{\kappa^2+1}]\}^2. \tag{A4}$$

From the Euler-MacLaurin formula (A2) one infers that, in contrast to case (a), apart from the integral on the rhs also the terms proportional to $F(1/2)$ and to $F'(1/2)$ have to be included in order to obtain the first three terms on the rhs of the expansion (2.32) of $\mathcal{C}_3(\tau)$. Proceeding in the same way as in case (a), one is led to consider modified Bessel functions I_a and K_a with order $a=\omega\sqrt{\tau}\sqrt{\kappa^2+1}$ and triple integrals over s, ω, and κ. One reproduces again the expression (2.35) for $\mathcal{C}_0$ and finds, using $B_2=1/6$, the expressions for $\mathcal{C}_1^{(3)}$ and $\mathcal{C}_2^{(3)}$ in Eq. (2.37).

(c) $d=2$. In this case the procedure is quite similar to that in case (b). The expression corresponding to (A1) now reads $F(0)/2+\Sigma_{n=1}^\infty F(n)$, where

$$F(n)=\tau\int_0^\infty d\kappa\,\kappa\frac{I_n(\sqrt{\tau}\sqrt{\kappa^2+1})}{K_n(\sqrt{\tau}\sqrt{\kappa^2+1})}\{K_n[(s+\sqrt{\tau})\sqrt{\kappa^2+1}]\}^2. \tag{A5}$$

The analysis shows that only the integral on the rhs of the Euler-MacLaurin formula (A2) contributes to the first three terms on the rhs of the expansion (2.32) of $\mathcal{C}_2(\tau)$ [compare cases (a) and (b) above]. One finds again the expression (2.35) for $\mathcal{C}_0$ and in addition the expressions for $\mathcal{C}_1^{(2)}$ and $\mathcal{C}_2^{(2)}$ in Eq. (2.38).

2. $\mathcal{C}_d(\tau)$ for $\tau\to 0$

The leading behavior of $C_d(\eta\to\infty)$ in Eq. (2.47) can be inferred from the behavior for $\tau\to 0$ of the quantity

$$\mathcal{I}_d(\tau)=-\frac{\tau^2}{8\pi^2}\mathcal{C}_d(\tau) \tag{A6}$$

with $\mathcal{C}_d(\tau)$ from Eq. (2.31). The behavior of $\mathcal{I}_d(\tau\to 0)$ exhibits two types of leading terms. The first is the logarithmically divergent contribution $-\alpha/(4\pi^2)\ln(1/\sqrt{\tau})$ which follows from the behavior $g_s(\psi,\tau,0)\to-\alpha/(4\pi^2)$ for $1\ll\psi\ll1/\sqrt{\tau}$ as mentioned below Eq. (2.15d). The second contribution is independent of τ and requires special care. Its evaluation is facilitated by splitting $\mathcal{I}_d(\tau)$ according to

$$\mathcal{I}_d(\tau)=\mathcal{H}_d(\tau)+\mathcal{J}_d(\tau), \tag{A7a}$$

where

$$\mathcal{H}_d(\tau)=\int_1^\infty d\psi\,\psi^{-1}\left\{\left[1-\psi^{-\alpha}\frac{K_\alpha(\psi\sqrt{\tau})}{K_\alpha(\sqrt{\tau})}\right]^2 g_s(\psi,\tau,0)\right.$$
$$\left.-g_s^{(\mathrm{as})}(\psi\sqrt{\tau},0)\right\}, \tag{A7b}$$

$$\mathcal{J}_d(\tau)=\int_1^\infty d\psi\,\psi^{-1}g_s^{(\mathrm{as})}(\psi\sqrt{\tau},0). \tag{A7c}$$

Here we have used Eqs. (2.9) and (2.12) and we have added and subtracted the function $g_s^{(\mathrm{as})}(\psi\sqrt{\tau},0)$, which is defined as in Eq. (2.15d), and represents the behavior of $g_s(\psi,\tau,0)$ for $1\ll\psi,\tau^{-1/2}$. In $\mathcal{H}_d$ one can interchange the order of the integration over ψ and the limit $\tau\to 0$ [62], which results in the finite limit

$$\mathcal{H}_d(\tau\to 0)\to\mathcal{B}_d=\int_1^\infty d\psi\,\psi^{-1}$$
$$\times\left\{[1-\psi^{-2\alpha}]^2\gamma_s(\psi,\varepsilon=0)+\frac{\alpha}{4\pi^2}\right\}, \tag{A8}$$

where the function

$$\gamma_s(\psi,\varepsilon)=g_s(\psi,\tau=0,\varepsilon) \tag{A9}$$

can be read off from Eq. (2.15b). The integral in Eq. (A8) is well-defined since $\gamma_s(\psi,0)$ tends to $-\alpha/(4\pi^2)$ for large ψ so that the logarithmic singularity is removed. The integral in Eq. (A7c) can be carried out explicitly and leads in conjunction with Eqs. (A7) and (A8) to

$$\mathcal{I}_d(\tau\to 0)\to\mathcal{B}_d+\frac{\alpha}{4\pi^2}\left[\frac{\ln\tau}{2}-\ln 2+1-\frac{\Psi(d/2)}{2}+\frac{C_E}{2}\right], \tag{A10}$$

where Ψ is the psi function and C_E denotes Euler's constant. Inserting Eq. (A10) in Eq. (A6) and carrying out the inverse Laplace transform in Eq. (2.31a) leads to the result for

TABLE II. Numerical values of $\ln \mathcal{C}_d(\tau)$ [see Eq. (2.31b)].

$\ln \tau$	$d=2$	$d=3$	$d=4$
-10	18.816	21.308	22.223
-9	16.795	19.175	20.108
-8	14.773	17.027	17.980
-7	12.755	14.865	15.835
-6	10.744	12.692	13.672
-5	8.748	10.511	11.488
-4	6.773	8.328	9.282
-3	4.830	6.160	7.057
-2	2.931	4.024	4.836
-1	1.085	1.946	2.640
0	-0.700	-0.054	0.504
1	-2.422	-1.966	-1.540

$Y_{d,D}(x \to \infty)$ in Eq. (2.48). We conclude this subsection by calculating the number $\mathcal{B}_d$ for $d=D$, $d=3$, and $d \searrow 2$ [see Eq. (2.50)].

(a) $d=D$. Since $\mathcal{I}_D$ belongs to the one-loop contribution of $Y_{D,D}$, we need to consider $\mathcal{I}_4$ only [compare the remarks below Eqs. (2.20) and (2.31b)]. This amounts to inserting $\alpha=1$ into Eq. (A8) and the function γ_s corresponding to a sphere in $D=4$ which is given by $\gamma_s(\psi,0)=-(4\pi^2)^{-1}[1-\psi^{-2}]^{-2}$ [63] yielding $\mathcal{B}_4=0$.

(b) $d=3$. For $2<d<D$ the quantity $\mathcal{B}_d$ does not vanish and can be evaluated numerically. For $d=3$ this leads to the value for $\mathcal{B}_3$ given in Eq. (2.50).

(c) $d \searrow 2$. In this limit $\mathcal{B}_d$ can be calculated exactly. It is useful to substitute $\sigma = \psi^{2\alpha}$ in Eq. (A8) and to carry out the limit $\alpha=(d-2)/2 \searrow 0$ for fixed σ in the ensuing integrand. One finds that only the term for $n=0$ in Eq. (2.15b) survives this limit with the result

$$\mathcal{B}_2 = \frac{1}{8\pi^2} \int_1^\infty d\sigma \, \sigma^{-1} \left\{ -\frac{\sigma-1}{\sigma} + 1 \right\} = \frac{1}{8\pi^2}. \quad \text{(A11)}$$

3. $\mathcal{C}_d(\tau)$ in the crossover region $0 \lesssim \tau \lesssim 3$

For the convenience of the reader, in Table II we give some numerical values of $\mathcal{C}_d(\tau)$. From these values an approximation for the full function $\mathcal{C}_d(\tau)$ can be constructed by using its asymptotic behaviors for $\tau \to \infty$ and $\tau \to 0$ as derived in the above subsections and by appropriate interpolation.

APPENDIX B: SMALL RADIUS EXPANSION TO ONE-LOOP ORDER

The relation (1.11) for polymers is—via the polymer magnet analogy—closely related to a corresponding small radius expansion (SRE) in a $(\mathbf{\Phi}^2)^2$ field theory with the Boltzmann weight $\exp(-\Delta \mathcal{H}_K\{\mathbf{\Phi}\})$ which describes the presence of the generalized cylinder K (compare Sec. II A and Appendix C). Here we shall illustrate the SRE by considering the two-point correlation function at the critical point of the field theory in one-loop order. This is particularly well suited to reveal the mechanism behind the SRE. Moreover, it provides a significant check for the operator character of the expan-

sion because we shall find the same small radius amplitude $A_{d,D}$ as in Sec. II C.

Keeping u and $\varepsilon=4-D$ as independent variables, the SRE can be written in the form

$$\exp(-\Delta \mathcal{H}_K) \propto 1 - \mathcal{F}(\mu R, u; \varepsilon, d)\mu^{2-d}Z_t \omega_K + \cdots \quad \text{(B1)}$$

with

$$\omega_K = \begin{cases} \int_{\mathbb{R}^\delta} d^\delta r_\parallel \mathbf{\Phi}^2(\mathbf{r}_\perp=0, \mathbf{r}_\parallel), & d<D \\ \mathbf{\Phi}^2(0), & d=D. \end{cases} \quad \text{(B2)}$$

Here $\mu^{2-d}Z_t \omega_K$ is a renormalized and dimensionless operator and

$$\mathcal{F}(\mu R, u; \varepsilon, d) = -\mathcal{A}_K^{(0)}(\mu R)^{d-2}[1 + uF_1(\mu R; \varepsilon, d) + O(u^2)] \quad \text{(B3)}$$

has an expansion in terms of u with the coefficient $-\mathcal{A}_K^{(0)} = 2\pi^{d/2}/\Gamma(\alpha) = \alpha\Omega_d$ of the leading term corresponding to the Gaussian model [see Eq. (4.6) in I]. The functions F_i can be expanded in terms of ε with coefficients which depend on μR only via powers of $\ln(\mu R)$. In particular, we shall find from the critical two-point function that

$$F_1(\mu R; \varepsilon, d) = \frac{\mathcal{N}+2}{3} \left[\ln(\mu R) + f_1 + e_d + \frac{4\pi^2}{\alpha}\mathcal{B}_d \right] + O(\varepsilon), \quad \text{(B4)}$$

where

$$e_d = 1 + \frac{\ln \pi}{2} - \frac{\Psi(d/2)}{2}; \quad \text{(B5)}$$

the quantity $\mathcal{B}_d$ has been introduced in Eq. (A8). The ellipses in Eq. (B1) stand for contributions in which higher powers of R are multiplied by powers of $\ln R$. Standard renormalization group arguments imply that for large μR the function $\mathcal{F}$ is proportional to $R^{d-1/\nu}$ and that the rhs of Eq. (B1) can be written as $1 + \mathcal{A}_K R^{d-1/\nu}\omega_K$, where

$$-\mathcal{A}_K = \mu^{2-1/\nu}Z_t D_L(u)\mathcal{F}(1, u^*; \varepsilon, d) \quad \text{(B6)}$$

with D_L from Eq. (2.28). The universal polymer amplitude $A_{d,D}$ in Eq. (1.11) is related to $\mathcal{A}_K = \mathcal{A}_K(\mathcal{N})$ via [64]

$$A_{d,D} = -\mathcal{A}_K(0)2\mu^{-2}Z_t^{-1}L\mathcal{R}_x^{-1/\nu}. \quad \text{(B7)}$$

By using Eq. (2.28) one finds that the nonuniversal quantities μ, Z_t, D_L, f_1 cancel and

$$A_{d,D} = \frac{2\pi^{d/2}}{\Gamma(\alpha)} \left\{ 1 + \frac{\varepsilon}{4}\left[\frac{4\pi^2}{\alpha}\mathcal{B}_d + \frac{3}{2} - \frac{\ln 2}{2} - \frac{\Psi(d/2)}{2} \right] + O(\varepsilon^2) \right\}, \quad \text{(B8)}$$

which indeed reproduces the first-order ε results of $A_{d,D}$ in Eq. (2.52).

We now verify Eqs. (B1)–(B5). Consider the two-point correlation function $\langle \Phi_j(\mathbf{r})\Phi_k(\mathbf{r}') \rangle$ of the field theory described by Eq. (2.6) at its critical point. For $u=0$ the SRE follows from the explicit expressions in Eq. (2.7) for the Gaussian propagator which by using Wick's theorem lead to

$$\langle \omega_K \Phi_j(\mathbf{r})\Phi_k(\mathbf{r}') \rangle_{b,[0]}$$

$$= \frac{\delta_{jk}}{2\pi^d}(r_\perp r'_\perp)^{-\alpha}\int_{\mathbb{R}^\delta}\frac{d^\delta P}{(2\pi)^\delta}\exp[i\mathbf{P}(\mathbf{r}_\parallel - \mathbf{r}'_\parallel)]$$

$$\times (P/2)^{2\alpha}K_\alpha(Pr_\perp)K_\alpha(Pr'_\perp)$$

$$= (\mathcal{A}_K^{(0)})^{-1}\lim_{R\to 0}R^{-2\alpha}\{\langle \Phi_j(\mathbf{r})\Phi_k(\mathbf{r}') \rangle_{[0]}$$

$$- \langle \Phi_j(\mathbf{r})\Phi_k(\mathbf{r}') \rangle_{b,[0]}\}. \quad (B9)$$

Here $\langle \rangle$ is a cumulant average with the subscript $[0]$ indicating $u=0$ and with b denoting the unbounded bulk space in the absence of K. Obviously Eq. (B9) verifies the SRE for the Gaussian model.

Consider now the first order in u contribution:

$$\langle \Phi_j(\mathbf{r})\Phi_k(\mathbf{r}') \rangle_{[1]} = -\delta_{jk}\frac{\mathcal{N}+2}{3}8\pi^2 f\mu^\varepsilon u R^{2\alpha}J(\mathbf{r},\mathbf{r}'), \quad (B10)$$

where

$$J(\mathbf{r},\mathbf{r}') = \int_{y_\perp > R}d^D y \; G(\mathbf{r},\mathbf{y};R)G(\mathbf{r}',\mathbf{y};R)I(y_\perp,R), \quad (B11)$$

$$I(y_\perp,R) = R^{-2\alpha}G(\mathbf{y},\mathbf{y};R)$$

$$= \frac{R^{-2\alpha}}{\mathcal{N}}\{\langle \mathbf{\Phi}^2(\mathbf{y})\rangle_{[0]} - \langle \mathbf{\Phi}^2(\mathbf{y})\rangle_{b,[0]}\}. \quad (B12)$$

The first order expression given in Eq. (B10) has the same structure as the one in Eq. (2.11) and we have used Eq. (2.16a). Note that in the present dimensional regularization scheme and at $t_0 = 0$ the bulk quantity $G_b(\mathbf{y},\mathbf{y}) = \langle \mathbf{\Phi}^2(\mathbf{y})\rangle_{b,[0]}/\mathcal{N}$ vanishes. We have exploited this in order to write the last expression in Eq. (B12) in such a form which allows us to make contact with Eq. (B9) and which implies

$$I(y_\perp,0) = \frac{\mathcal{A}_K^{(0)}}{\mathcal{N}}\langle \omega_K \mathbf{\Phi}^2(\mathbf{y})\rangle_{b,[0]}$$

$$= -y_\perp^{-d+\varepsilon}\frac{\alpha}{4\pi^2}\{1 + \varepsilon e_d + O(\varepsilon^2)\}. \quad (B13)$$

The function $I(y_\perp,R)$ is related to $\gamma_s(\psi,\varepsilon)$ in Eq. (A9) by

$$y_\perp^{d-\varepsilon}I(y_\perp,R) = \gamma_s(y_\perp/R,\varepsilon), \quad (B14)$$

and Eq. (B13) is consistent with $\gamma_s(\infty,0) = -\alpha/(4\pi^2)$ as mentioned below Eq. (A9). In order to verify Eqs. (B1)–(B5) we decompose $J(\mathbf{r},\mathbf{r}')$ according to

$$J = J_{(i)} + J_{(ii)} + J_{(iii)} \quad (B15)$$
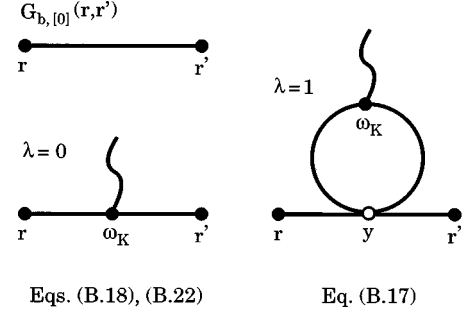

Eqs. (B.18), (B.22)   Eq. (B.17)

FIG. 5. Representation of $\langle \omega_K \Phi_1(\mathbf{r})\Phi_1(\mathbf{r}')\rangle_{b,[\lambda]}$ appearing on the right-hand side of Eqs. (B17), (B18), and (B22). The solid lines correspond to the bulk Gaussian propagator $G_{b,[0]} \equiv G_b$ and $\lambda = 0,1$ denotes the loop order. The wiggly lines indicate the insertion of the operator ω_K located at the "axis" of the generalized cylinder K.

with

$$J_{(i)}(\mathbf{r},\mathbf{r}') = \int_{\mathbb{R}^D}d^D y \; G_b(\mathbf{r},\mathbf{y})G_b(\mathbf{r}',\mathbf{y})I(y_\perp,R=0), \quad (B16a)$$

$$J_{(ii)}(\mathbf{r},\mathbf{r}') = -\int_{0 < y_\perp < R}d^D y \; G_b(\mathbf{r},\mathbf{y})G_b(\mathbf{r}',\mathbf{y})I(y_\perp,R=0), \quad (B16b)$$

$$J_{(iii)}(\mathbf{r},\mathbf{r}') = \int_{y_\perp > R}d^D y \; \{G(\mathbf{r},\mathbf{y};R)G(\mathbf{r}',\mathbf{y};R)I(y_\perp,R)$$

$$- G_b(\mathbf{r},\mathbf{y})G_b(\mathbf{r}',\mathbf{y})I(y_\perp,R=0)\}. \quad (B16c)$$

In the following we analyze the behavior of the rhs of Eq. (B10) for $R \to 0$ which arises from each of these contributions $J_{(i)}$, $J_{(ii)}$, and $J_{(iii)}$.

Rewriting $I(y_\perp,0)$ in the integrand on the rhs of Eq. (B16a) by means of the first equality in Eq. (B13) one finds (see Fig. 5)

$$\langle \Phi_j(\mathbf{r})\Phi_k(\mathbf{r}') \rangle_{[1],(i)} \to \mathcal{A}_K^{(0)}R^{2\alpha}\langle \omega_K \Phi_j(\mathbf{r})\Phi_k(\mathbf{r}') \rangle_{b,[1]}. \quad (B17)$$

In order to evaluate the leading contribution of $J_{(ii)}$ for small R, one can set $\mathbf{y}_\perp = \mathbf{0}$ in the two bulk propagators $G_b(\mathbf{r},\mathbf{y})$ and $G_b(\mathbf{r}',\mathbf{y})$ in the integrand on the rhs of Eq. (B16b). Its remaining dependence on $y_\perp$ as given by the last expression in Eq. (B13) leads to a pole in ε. This results in (see Fig. 5)

$$\langle \Phi_j(\mathbf{r})\Phi_k(\mathbf{r}') \rangle_{[1],(ii)}$$

$$\to \mathcal{A}_K^{(0)}R^{2\alpha}\langle \omega_K \Phi_j(\mathbf{r})\Phi_k(\mathbf{r}') \rangle_{b,[0]}$$

$$\times \left\{(Z_t)_{[1]} + \frac{\mathcal{N}+2}{3}u[\ln(\mu R) + f_1 + e_d]\right\}, \quad (B18)$$

where $(Z_t)_{[1]} = (\mathcal{N}+2)u/(3\varepsilon)$ is the contribution to Z_t of first order in u [see Eq. (2.16b)].

For the leading contribution of $J_{(iii)}$ for $R \to 0$, it is sufficient to confine the integration over $\mathbf{y}_\perp$ on the rhs of Eq. (B16c) to the restricted region $R < y_\perp < \sqrt{Rr_\perp^{(<)}}$ with $r_\perp^{(<)} = \min(r_\perp, r'_\perp)$. The reason is that in the remaining integration

region not only the ratios $R/r_\perp$ and $R/r_\perp'$ but also $R/y_\perp$ are small so that in leading order one can insert $R=0$ into the first term in curly brackets, which is then canceled by the second term. In particular, in the restricted region $y_\perp$ is smaller than $r_\perp$ and $r_\perp'$. By inserting the representation (2.7) for the external legs G and G_b in Eq. (B16c), one finds that only the terms for $n=0$ contribute to the leading behavior of $J_{(iii)}$ for which one obtains

$$J_{(iii)}(\mathbf{r},\mathbf{r}') \to \frac{\Omega_d}{2} R^\varepsilon \langle \omega_K \Phi_1(\mathbf{r})\Phi_1(\mathbf{r}') \rangle_{b,[0]} \beta_d, \quad (B19)$$

$$\beta_d = \int_1^\infty d\psi \, \psi^{-1+\varepsilon} \{ [1-\psi^{-2\alpha}]^2 \gamma_s(\psi,\varepsilon) - \gamma_s(\infty,\varepsilon) \} \quad (B20)$$

with γ_s from Eq. (B14). The quantity β_d arises as the limit for $R \to 0$ of the expression [65]

$$\int_1^{\sqrt{r_\perp^{(<)}/R}} d\psi \, \psi^{-1+\varepsilon} [\Gamma(\alpha+1)]^2 \left(\frac{RP\psi}{2}\right)^{-2\alpha} \left\{ \left[I_\alpha(RP\psi) - \frac{I_\alpha(RP)}{K_\alpha(RP)} K_\alpha(RP\psi) \right]^2 \gamma_s(\psi,\varepsilon) - [I_\alpha(RP\psi)]^2 \gamma_s(\infty,\varepsilon) \right\}. \quad (B21)$$

Of course, $\beta_d \to \mathcal{B}_d$ for $\varepsilon \to 0$ and the present procedure for $R/r_\perp^{(<)} \to 0$ at the critical point of the field theory leading to Eq. (B20) should be compared with the procedure for $R/\xi_+ \to 0$ leading to $\mathcal{B}_d$ in Eq. (A8). Equation (B19) implies (see Fig. 5)

$$\langle \Phi_j(\mathbf{r})\Phi_k(\mathbf{r}') \rangle_{[1],(iii)} \to \mathcal{A}_K^{(0)} R^{2\alpha} \langle \omega_K \Phi_j(\mathbf{r})\Phi_k(\mathbf{r}') \rangle_{b,[0]} \frac{\mathcal{N}+2}{3} u \frac{4\pi^2}{\alpha} \mathcal{B}_d + O(u\varepsilon). \quad (B22)$$

Equations (B17), (B18), and (B22) corroborate the SRE in Eqs. (B1)—(B5) to first order in u in the case of the critical correlation function. Note the recurrent character of the SRE which is typical for operator product expansions [37(b)]. A graphical representation of the bulk correlation function with insertion of the operator ω_K is shown in Fig. 5.

Apart from particles in a polymer solution, there are other physical systems the SRE can be applied to such as spherical or cylindrical particles in liquid ^{4}He near the λ point and nonmagnetic inclusions in a ferromagnet of Ising or Heisenberg type near the Curie point. For these systems the parameter $\mathcal{N}$ takes the values 2, 1, and 3, respectively. A useful characterization of the small sphere or the thin cylinder in these cases is provided by the universal amplitude

$$\hat{A}_{d,D}(\mathcal{N}) = -\mathcal{A}_K(\mathcal{N}) \sqrt{\frac{B_{\Phi^2}(\mathcal{N})}{\mathcal{N}}} \quad (B23)$$

with the amplitude B_{Φ^2} of the bulk correlation function $\langle \mathbf{\Phi}^2(\mathbf{r})\mathbf{\Phi}^2(0) \rangle_b = B_{\Phi^2} r^{-2(D-1/\nu)}$ at the critical point. For example, the change in free energy per unit "length" l^δ which arises upon immersing the generalized cylinder K into the bulk system displays a singular dependence on $t \sim (T-T_c)/T_c$ given by

$$\left[-\frac{k_B T}{l^\delta} \ln \langle e^{-\Delta\mathcal{H}_K} \rangle_{b,t} \right]_{\text{sing}}$$

$$= -k_B T_c R^{d-1/\nu} \mathcal{A}_K(\mathcal{N}) [\langle \mathbf{\Phi}^2 \rangle_{b,t}]_{\text{sing}}$$

$$= k_B T_c R^{d-1/\nu} \xi^{-(D-1/\nu)} \hat{A}_{d,D}(\mathcal{N}) \hat{E}(\mathcal{N}) \quad (B24)$$

with the universal bulk amplitude

$$\hat{E}(\mathcal{N}) = [\langle \mathbf{\Phi}^2 \rangle_{b,t}]_{\text{sing}} \xi^{D-1/\nu} (B_{\Phi^2}/\mathcal{N})^{-1/2}, \quad (B25)$$

which characterizes the temperature dependence of the bulk energy density. From Eqs. (B1)–(B6) and from the dependence of $B_{\Phi^2}(\mathcal{N})$ on ε one obtains the following explicit expressions:

$$\hat{A}_{D,D}(\mathcal{N}) = \frac{1}{\sqrt{2}} + O(\varepsilon^2), \quad (B26a)$$

$$\hat{A}_{3,D}(\mathcal{N}) = \frac{1}{\sqrt{2}\pi} \left\{ 1 + \frac{\varepsilon}{2} \left[C_E + \ln \pi + \frac{\mathcal{N}+2}{\mathcal{N}+8} \right. \right.$$
$$\left. \left. \times (16\pi^2 \mathcal{B}_3 + 2\ln 2 - 1) \right] \right\} + O(\varepsilon^2), \quad (B26b)$$

and

$$\hat{A}_{2,D}(\mathcal{N}) = \varepsilon \frac{\mathcal{N}+2}{\mathcal{N}+8} 2^{3/2} \pi \mathcal{B}_2 + O(\varepsilon^2). \quad (B26c)$$

The first-order ε result (B26a), which we have obtained by carrying out the calculation *directly* in the outer space of a sphere, confirms the prediction [34]

$$\hat{A}_{D,D}(\mathcal{N}) = \sqrt{(A_O^{\Phi^2})^2/(\mathcal{N}B_{\Phi^2})}, \quad (B27)$$

which follows from relating the half-space (hs) profile $\langle \mathbf{\Phi}^2(z) \rangle_{\text{hs}} = A_O^{\Phi^2}(2z)^{-(D-1/\nu)}$ with the distance z from a planar wall with Dirichlet boundary conditions O at the bulk critical point to the profile $\langle \mathbf{\Phi}^2(r) \rangle$ in the outer space of the sphere by means of a conformal transformation [60] [for $\mathcal{N}=1$ compare the explicit result in the first Eq. (20) of Ref. [34(a)]. The consistency of the above results is expected but remarkable since the finite conformal map changes the geometry under consideration.

It is helpful to summarize the relationship between the universal amplitude $A_{d,D}$ for polymers and the universal amplitude $\hat{A}_{d,D}$ for the field theory in terms of the symbolic equation

$$A_{d,D}\Psi = \hat{A}_{d,D}\sqrt{\mathcal{N}/B_{\Phi^2}}\Phi^2, \qquad (B28)$$

which applies inside averages or correlation functions for $\mathcal{N}\searrow 0$ with Ψ defined in Eq. (C7). Since $\Psi = \sqrt{b_\Psi/B_{\Phi^2}}\Phi^2$, with $b_\Psi = [\mathcal{R}_x^{1/\nu}/(2L_0)]^2 B_{\Phi^2}$ from Eq. (C10), one has

$$A_{d,D} = (\hat{A}_{d,D}\sqrt{\mathcal{N}/b_\Psi})_{\mathcal{N}\searrow 0}. \qquad (B29)$$

For a spherical particle, in particular, the polymer amplitude $A_{D,D}$ can be expressed in terms of the critical universal amplitude ratio on the rhs of Eq. (B27) and the noncritical universal bulk amplitude b_Ψ. In $D=2$ both are explicitly known [19(b)] and lead to the value $A_{2,2}=3.81$ in Table I.

APPENDIX C: SHORT DISTANCE AMPLITUDE FOR POLYMER DENSITY CORRELATIONS

Here we calculate the universal amplitude σ in Eqs. (3.5) and (3.6). While for $D=4$ it coincides with the corresponding ideal chain value $\sigma^{(id)}=\pi^{-2}$ from Eq. (3.7), in $D=3$, 2, and 1 the amplitude σ is different from $\sigma^{(id)}$.

(a) $D=3$. In this case results are available [18,49] for the normalized scattering form factor $H(Q)$ which is defined for general D by

$$C_2(\mathbf{r},0) = \mathcal{R}_x^{2/\nu}\int_{\mathbb{R}^D}\frac{d^D Q}{(2\pi)^D}\exp(i\mathbf{Q}\cdot\mathbf{r})H(Q), \qquad (C1)$$

where $H(0)=1$ as implied by Eq. (3.3). The amplitude h_∞ in the power law

$$H(Q\to\infty)\to h_\infty(Q^2\mathcal{R}_x^2/2)^{-1/(2\nu)} \qquad (C2)$$

is related to σ by

$$\sigma = h_\infty 2^{-1/(2\nu)}\pi^{-D/2}\Gamma\left(\frac{D-1/\nu}{2}\right)\Big/\Gamma\left(\frac{1}{2\nu}\right). \qquad (C3)$$

From the accepted [18,49] approximate value $h_\infty \approx 1.1$ in $D=3$, one infers via Eq. (C3) the value $\sigma \approx 0.13$ (see Table I).

(b) $D=2$. In this case one can obtain a fairly accurate estimate for σ by combining a numerical estimate for a ratio of gyration radii of ring- and open-chain polymers with conformal invariance and Bethe ansatz results for the $O(\mathcal{N})$ vector model by invoking the polymer magnet analogy (PMA) [15,17]. By using the language of the Ginzburg-Landau field theory (compare Sec. II A) the necessary relations of the PMA can be written in a way which makes the generalization to $D=2$ obvious. The polymer average

$$\{\rho(\mathbf{r}_A)\rho(\mathbf{r}_B)\rho(\mathbf{r}_C)\}_\mathbf{y}$$

$$= \frac{\mathcal{L}\left\langle \Psi(\mathbf{r}_A)\Psi(\mathbf{r}_B)\Psi(\mathbf{r}_C)\Phi_1(\mathbf{y})\int d^D y' \Phi_1(\mathbf{y}')\right\rangle}{\mathcal{L}\left\langle \Phi_1(\mathbf{y})\int d^D y' \Phi_1(\mathbf{y}')\right\rangle} \qquad (C4)$$

is expressed in terms of cumulant averages $\langle\,\rangle$ of the field theory. Here $\mathcal{L}=\mathcal{L}(t_0\to L_0)$ denotes an inverse Laplace transform defined as in Eq. (2.5) and relates the strength t_0 in the thermal perturbation

$$\mathcal{H}_{th} = \int_{\mathbb{R}^D}d^D r\, \mathcal{T}(\mathbf{r}), \qquad (C5)$$

$$\mathcal{T}(\mathbf{r}) = \frac{t_0}{2}\Phi^2(\mathbf{r}), \qquad (C6)$$

of the Hamiltonian *at* the critical point of the field theory to the bare ''chain length'' L_0 which—apart from a nonuniversal proportionality factor—equals the number of monomers in the polymer chain. The scaling dimension of the quantity

$$\Psi(\mathbf{r}) = \mathcal{R}_x^{1/\nu}\frac{1}{E}\mathcal{T}(\mathbf{r}) \qquad (C7)$$

equals its inverse length dimension $D-1/\nu$. Here $E=t_0 L_0$ is the exponent which appears in $\mathcal{L}$ [compare Eq. (2.5)]. The rhs of Eq. (C4) has the normalization property that by integrating the numerator over, say, $\mathbf{r}_A$ one can replace $\int d^D r_A \Psi(\mathbf{r}_A)$ by $\mathcal{R}_x^{1/\nu}$ [compare the discussion related to Eq. (18) in Ref. [57]]. This is consistent with the corresponding normalization property $\int d^D r_A \rho(\mathbf{r}_A) = \mathcal{R}_x^{1/\nu}$ for the lhs of Eq. (C4) as implied by Eq. (1.13).

Short distance properties such as those in Eqs. (3.5) and (3.6) follow from the operator product expansion (OPE)

$$\Psi(\mathbf{r}_A)\Psi(\mathbf{r}_B) \to \sigma r_{AB}^{-(D-1/\nu)}\Psi[(\mathbf{r}_A+\mathbf{r}_B)/2], \qquad (C8)$$

which is equivalent to the well-known OPE of energy density operators [37(b),59]. The amplitude σ is expressed as

$$\sigma = \zeta\sqrt{b_\Psi}. \qquad (C9)$$

Here b_Ψ is the universal bulk amplitude in

$$\langle\Psi(\mathbf{r})\Psi(0)\rangle_{\text{crit}} = b_\Psi r^{-2(D-1/\nu)} \qquad (C10)$$

with $\langle\,\rangle_{\text{crit}}$ denoting the average at the critical point of the field theory and ζ is the amplitude which replaces σ in the corresponding OPE for the normalized energy density $\tilde{\Psi} = \Psi/\sqrt{b_\Psi}$. By using results of Refs. [66,67] one finds that in $D=2$ for $\mathcal{N}\searrow 0$,

$$\mathcal{N}^{1/2}\zeta \to (216\pi)^{1/2}\left|\frac{\Gamma(2/3)}{\Gamma(1/3)}\right|^{9/2} \approx 1.21 \qquad (C11)$$

[compare Eq. (7.161) in Ref. [19(a)], where ζ is denoted by c_2]. The amplitude b_Ψ has been calculated in the Appendix of Ref. [19(b)] by using results of Ref. [68] so that in $D=2$ for $\mathcal{N}\searrow 0$ one has

$$\mathcal{N}^{-1/2}\sqrt{b_\Psi} \to \frac{\kappa}{\pi}\left(\frac{5}{6}\mathcal{R}_x^2 \bigg/ \mathcal{R}_{\rm ring}^2\right)^{2/3}, \qquad (C12)$$

where $\kappa = 0.226\,630$ and $\mathcal{R}_x^2/\mathcal{R}_{\rm ring}^2 \approx 6.85$ [69] is the ratio of $\mathcal{R}_x^2$ of an open polymer chain and the mean square radius of gyration $\mathcal{R}_{\rm ring}^2 = \mathcal{R}_{x,{\rm ring}}^2 + \mathcal{R}_{y,{\rm ring}}^2$ of a *ring polymer* with the

same number of monomers. Equations (C9)–(C12) lead to the value $\sigma \approx 0.278$ in Table I.

(c) $D = 1$. In this case the behavior of a chain with excluded volume interaction is that of a rigid rod of length $\mathcal{R}_x$. Thus $\nu = 1$ and $C_2(\mathbf{r},0)$ equals $\mathcal{R}_x - |\mathbf{r}|$ for $|\mathbf{r}| \leqslant \mathcal{R}_x$ while it vanishes for $|\mathbf{r}| > \mathcal{R}_x$. The assumption that Eq. (3.5) still holds for $D = 1$ leads to the value $\sigma = 1$ in Table I.

---

[1] *Colloid Physics*, Proceedings of the Workshop on Colloid Physics, University of Konstanz, Germany, 1995 [Physica A **235** (1997)].

[2] P. R. Sperry, H. B. Hopfenberg, and N. L. Thomas, J. Colloid Interface Sci. **82**, 62 (1980).

[3] R. Verma, J. C. Crocker, T. C. Lubensky, and A. G. Yodh, Phys. Rev. Lett. **81**, 4004 (1998).

[4] Y. N. Ohshima *et al.*, Phys. Rev. Lett. **78**, 3963 (1997); D. Rudhardt, C. Bechinger, and P. Leiderer, *ibid.* **81**, 1330 (1998).

[5] S. Asakura and F. Oosawa, J. Chem. Phys. **22**, 1255 (1954); J. Polym. Sci. **33**, 183 (1958). Based on ideas in these pioneering papers, an approximate polymer-particle interaction has been introduced for the case in which the polymer size is small compared with the particle size by considering the polymer as a hard sphere (PHS) with a fixed radius of the order of the Flory radius; see, e.g., A. Vrij, Pure Appl. Chem. **48**, 471 (1976); H. de Hek and A. Vrij, J. Colloid Interface Sci. **84**, 409 (1981).

[6] J. F. Joanny, L. Leibler, and P. G. de Gennes, J. Polym. Sci., Polym. Phys. Ed. **17**, 1073 (1979).

[7] P. G. de Gennes, C. R. Acad. Sci. (Paris) **288B**, 359 (1979).

[8] T. Odijk, Macromolecules **29**, 1842 (1996); J. Chem. Phys. **106**, 3402 (1996).

[9] Excluded volume effects for dilute or semidilute solutions of free polymers interacting with colloidal particles have been investigated by means of integral equation techniques; see, e.g., (a) M. R. Shaw and D. Thirumalai, Phys. Rev. A **44**, 4797 (1991); (b) A. Yethiraj, C. K. Hall, and R. Dickman, J. Colloid Interface Sci. **151**, 102 (1992); (c) P. G. Khalatur, L. V. Zherenkova, and A. R. Khokhlov, Physica A **247**, 205 (1997). For computer simulations in the case of a semidilute polymer solution, see (d) R. Dickman and A. Yethiraj, J. Chem. Phys. **100**, 4683 (1994).

[10] J. F. Joanny, J. Phys. (France) **49**, 1981 (1988).

[11] K. M. Jansons and C. G. Phillips, J. Colloid Interface Sci. **137**, 75 (1990).

[12] E. J. Meijer and D. Frenkel, J. Chem. Phys. **100**, 6873 (1994).

[13] R. Lipowsky, Europhys. Lett. **30**, 197 (1995).

[14] E. Eisenriegler, A. Hanke, and S. Dietrich, Phys. Rev. E **54**, 1134 (1996). In the main text this reference will be denoted as I.

[15] P. G. de Gennes, *Scaling Concepts in Polymer Physics* (Cornell University Press, Ithaca, 1979).

[16] We use the phrase ''excluded volume interaction'' exclusively for the repulsive interaction between chain monomers and not for the interaction between a colloidal particle and a chain monomer.

[17] J. des Cloizeaux and G. Jannink, *Polymers in Solution* (Clarendon, Oxford, 1990).

[18] L. Schäfer, *Excluded Volume Effects in Polymer Solutions as Explained by the Renormalization Group* (Springer, Heidelberg, 1999).

[19] (a) E. Eisenriegler, *Polymers near Surfaces* (World Scientific, Singapore, 1993); (b) in *Field Theoretical Tools in Polymer and Particle Physics*, edited by H. Meyer-Ortmanns and A. Klümper, Lecture Notes in Physics Vol. 508 (Springer, Heidelberg, 1998).

[20] For a review, see, e.g., U. Seifert and R. Lipowsky, in *Structure and Dynamics of Membranes*, edited by R. Lipowsky and E. Sackmann (Elsevier, Amsterdam, 1995), Vol. 1.

[21] Y. Jayalakshmi and E. W. Kaler, Phys. Rev. Lett. **78**, 1379 (1997).

[22] P. A. Buining, A. P. Philipse, and H. N. W. Lekkerkerker, Langmuir **10**, 2106 (1994).

[23] F. Gittes, B. Mickey, J. Nettleton, and J. Howard, J. Cell Biol. **120**, 923 (1993).

[24] The superscript (1) stands for one-body contribution (compare Sec. I C).

[25] (a) P. G. de Gennes, J. Phys. Chem. **94**, 8407 (1990); (b) R. Balian and C. Bloch, Ann. Phys. (N.Y.) **60**, 401 (1970); **64**, 271 (1971); **84**, 559 (1974); (c) B. Duplantier, Physica A **168**, 179 (1990).

[26] F. David, in *Statistical Mechanics of Membranes and Surfaces*, edited by D. Nelson, T. Piran, and S. Weinberg (World Scientific, Singapore, 1988).

[27] W. Helfrich, Z. Naturforsch. C **28**, 693 (1973).

[28] K. Yaman, P. Pincus, and C. M. Marques, Phys. Rev. Lett. **78**, 4514 (1997); K. Yaman, M. Jeng, P. Pincus, C. Jeppesen, and C. M. Marques, Physica A **247**, 159 (1997).

[29] H.-G. Döbereiner, E. Evans, M. Kraus, U. Seifert, and M. Wortis, Phys. Rev. E **55**, 4458 (1997).

[30] Throughout this work we treat the actual common solvent of the particles and the polymers as an inactive background medium so that without polymers the dilute particles behave as an ideal gas. In the context of Eq. (1.10) the ''solvent'' of the particles is formed by the polymers which are separated from the ideal gas phase of the particles, e.g., by a semipermeable membrane.

[31] Examples for such lengths are the distances from the particle of a fixed end of the chain, of specific points of the local monomer density distribution of the chain, or of another boundary which is impenetrable for the chain.

[32] Since the particle is impenetrable and acts upon each monomer of the chain with a hard repulsive potential V_K, the Boltzmann weight $W_K\{\mathbf{y}_i\} = \exp[-V_K\{\mathbf{y}_i\}/k_B T]$ equals one for chain configurations $\{\mathbf{y}_i\}$ that do not intersect the particle and equals zero otherwise.

[33] The interaction of a self-avoiding walk with a cylinder of *microscopic* radius (needle) in three dimensions also gives rise to the exponent $d - 1/\nu = 2 - 1/\nu$ [compare S. Caracciolo, M. S. Causo, and A. Pelissetto, J. Phys. A **30**, 4939 (1997)], but cannot be characterized by the universal amplitude $A_{d,D} = A_{2,3}$.

[34] (a) T. W. Burkhardt and E. Eisenriegler, Phys. Rev. Lett. **74**, 3189 (1995); (b) E. Eisenriegler and U. Ritschel, Phys. Rev. B **51**, 13 717 (1995).

[35] K. Binder, in *Phase Transitions and Critical Phenomena*, edited by C. Domb and J. L. Lebowitz (Academic, London, 1983), Vol. 8, p. 1.

[36] H. W. Diehl, in *Phase Transitions and Critical Phenomena*, edited by C. Domb and J. L. Lebowitz (Academic, London, 1986), Vol. 10, p. 75; H. W. Diehl, Int. J. Mod. Phys. B **11**, 3503 (1997).

[37] (a) D. J. Amit, *Field Theory, the Renormalization Group, and Critical Phenomena* (McGraw-Hill, New York, 1978); (b) J. Zinn-Justin, *Quantum Field Theory and Critical Phenomena* (Clarendon, Oxford, 1989).

[38] (a) M. Abramowitz and I. A. Stegun, *Handbook of Mathematical Functions* (Dover, New York, 1972); (b) I. S. Gradshteyn and I. M. Ryzhik, *Table of Integrals, Series, and Products* (Academic, London, 1965).

[39] For the renormalization in the presence of curved surfaces, see K. Symanzik, Nucl. Phys. B **190**, 1 (1981).

[40] For a table of inverse Laplace transforms see, e.g., *Tables of Integral Transforms*, edited by A. Erdélyi (McGraw-Hill, New York, 1954), Vol. I.

[41] A bending of the membrane surface towards the solution also occurs for *rigid* nonadsorbing particles instead of polymers; see, e.g., R. Lipowsky and H.-G. Döbereiner, Europhys. Lett. **43**, 219 (1998).

[42] The dashed line in Fig. 2 is known rather accurately by means of the ε expansion of $\nu(D)$ in conjunction with the exact value of $\nu(D=2)$ [37].

[43] For example, for $(d,D)=(2,4)$ and ideal chains the reduced free energy increase $n_p f_K^{(1)}$ vanishes for $R \to 0$ as $\sim \mathcal{R}_x^2 / \ln(\mathcal{R}_x/R)$ [10] involving a logarithm which should be compared with the power-law decay $\sim \mathcal{R}_x^{1/\nu} R^{2-1/\nu}$ with $1/\nu \approx 1.7$ for chains with EV interaction in $(d,D)=(2,3)$.

[44] Methods based on conformal invariance allow one to reduce $A_{D,D}$ for arbitrary D to a half-space amplitude [60] and, for the particular dimension $D=2$, even to a bulk amplitude [67]. The latter can be evaluated by using Bethe ansatz results [68] and the ratio $\mathcal{R}_x/\mathcal{R}_{\text{ring}}$ considered in Eq. (C12).

[45] Compare G. Flöter and S. Dietrich, Z. Phys. B **97**, 213 (1995).

[46] R. P. Sear, Phys. Rev. E **57**, 1983 (1998).

[47] For a review see G. Fleer, M. Cohen-Stuart, J. Scheutjens, T. Cosgrove, and B. Vincent, *Polymers at Interfaces* (Chapman and Hall, London, 1993).

[48] The problem of the effective interaction between a *line* perturbation and a planar wall in a critical Gaussian field theory has been considered by H. Li and M. Kardar, Phys. Rev. A **46**, 6490 (1992). These authors find that it is necessary to introduce explicit regularization cutoffs which are nonuniversal parameters. However, in a critical $(\Phi^2)^2$ field theory in $D=3$ such regularization cutoffs are not necessary because in this case the small radius expansion for the field theory applies (see Appendix B), resulting in a universal dependence of the effective interaction on $\mathcal{D}$ and R.

[49] B. Duplantier, J. Phys. (Paris) **47**, 1633 (1986).

[50] The anisotropy of the dumbbell becomes visible only beyond the leading order.

[51] Here one may replace the sum in Eq. (3.18a) by an integral according to the Euler-MacLaurin formula in Eq. (A2) where

[52] A detailed discussion of the polymer depletion interaction between a spherical particle and a planar wall is given in A. Bringer, E. Eisenriegler, F. Schlesener, and A. Hanke, Eur. Phys. J. B (to be published).

[53] The Derjaguin expression of the free energy of interaction between two large spheres with the same radius R follows from the corresponding free energy between a sphere and a planar wall in Eq. (14) in Ref. [57] by replacing the prefactor R with $R/2$. The reason is a corresponding replacement in the local distance $\tilde{D}(r_\parallel)$ in Ref. [57].

[54] For $N=100$ our crude estimate is off by only 20%. The reason for the larger deviation in the case of $N=10$ could be that $N=10$ is still too small for a comparison with the universal asymptotics.

[55] A discussion of the validity of the PHS model in the case of the solvation free energy for a single particle is given in I.

[56] The effective radius $\tilde{\mathcal{R}}$ of the polymer ''spheres'' may be adjusted to $\mathcal{R}_x$ by comparing the free energy change on immersing a single large sphere in the unbounded solution. This leads to $\tilde{\mathcal{R}} = \sqrt{2/\pi} \mathcal{R}_x$ [compare Eq. (3.10) in I].

[57] E. Eisenriegler, Phys. Rev. E **55**, 3116 (1997).

[58] K. R. Myers, M. Nemirovsky, and K. F. Freed, J. Chem. Phys. **97**, 2790 (1992).

[59] J. L. Cardy, in *Phase Transitions and Critical Phenomena*, edited by C. Domb and J. L. Lebowitz (Academic, London, 1986), Vol. 11, p. 55.

[60] T. W. Burkhardt and E. Eisenriegler, J. Phys. A **18**, L83 (1985).

[61] C. M. Bender and S. A. Orszag, *Advanced Mathematical Methods for Scientists and Engineers* (McGraw-Hill, New York, 1978).

[62] The function $g_s^{(\text{as})}(\psi\sqrt{\tau},0)$ has the property that the integral in Eq. (A7b) is dominated by contributions from the ψ interval $1 < \psi < \varphi$ with $1 \ll \varphi \ll \tau^{-1/2}$. Alternatively, we observe that the integrand in Eq. (A7b) approaches its limit for $\tau \to 0$ uniformly with respect to ψ (compare section 6.2 in Ref. [61]).

[63] E. Eisenriegler, Z. Phys. B **61**, 299 (1985).

[64] Compare Eq. (4.8) in I where $A_{d,D}$ is denoted by $-\tilde{\mathcal{A}}_K D^{(1/2\nu)-1}$ and where the bare ''chain length'' $L_0 = \mu^{-2} Z_t^{-1} L$ is denoted by L. See also the argument in Ref. [19(b)] according to which $A_{d,D}$ can be read off by rewriting the right-hand side of Eq. (B1) for large μR as $1 - A_{d,D} R^{d-1/\nu} \tilde{\omega}_K$, where $\tilde{\omega}_K$ follows from ω_K in Eq. (B2) upon replacing Φ^2 by Ψ as defined in Eq. (C7).

[65] The square of the large square bracket in the expression (B21) is one of the factors which arises in the product $\tilde{G}_0(r_\perp, y_\perp; P^2, R) \tilde{G}_0(r'_\perp, y_\perp; P^2, R)$ [see Eq. (2.7c)]. By calculating the right-hand side of Eq. (B16c), the remaining factor and the integration over $\mathbf{P}$ (which replaces the integration over $\mathbf{y}_\parallel$ of Fourier transformed quantities) lead to an integral over $\mathbf{P}$ identical to the one in Eq. (B9). This gives rise to the factor $\langle \omega_K \Phi_1(\mathbf{r}) \Phi_1(\mathbf{r}') \rangle_{b,[0]}$ in Eq. (B19).

[66] V. S. Dotsenko and V. A. Fateev, Nucl. Phys. B **240**, 312 (1984); **251**, 691 (1985).

[67] T. W. Burkhardt, E. Eisenriegler, and I. Guim, Nucl. Phys. B **316**, 559 (1989).

[68] J. Cardy and G. Mussardo, Nucl. Phys. B **410**, 451 (1993).

[69] J. L. Cardy and A. J. Guttmann, J. Phys. A **26**, 2485 (1993).